Research Square

Preprints are preliminary reports that have not undergone peer review.
They should not be considered conclusive, used to inform clinical practice,
or referenced by the media as validated information.

Reduced hippocampal cysteine levels in adult offspring is associated with hippocampal and behavioral impairments induced by maternal $PM_{2.5}$ exposure

Suk-Yu Yau

sonata.yau@polyu.edu.hk

The Hong Kong polytechnic university https://orcid.org/0000-0002-7425-6741

Yunxiao Yunxiao Zhong
Akhlaq Hussain
Cheng Tong
Ahadullah -
Julia Rosa
Danyue Danyue Zhao
Shicong Du
Patrick K H Lee
JIASUI YU

HongKong polytechnic university https://orcid.org/0000-0001-6318-0393

Douglas Formolo
Yvonne Han
Chetwyn Chan
Hai Guo
Yang yang

Article

Keywords: PM2.5, maternal exposure, hippocampal impairments, offspring, synaptic plasticity, metabolites

Posted Date: June 1st, 2026

DOI: https://doi.org/10.21203/rs.3.rs-8854068/v1

License: This work is licensed under a Creative Commons Attribution 4.0 International License.
Read Full License

Additional Declarations: The authors have declared there is **NO** conflict of interest to disclose

Abstract

Neurodevelopmental disorders are influenced by genetic and environmental factors, with air pollution emerging as a significant risk factor. This study investigates the impact of maternal exposure to $PM_{2.5}$ on hippocampal plasticity of offspring. To mimic continuous maternal $PM_{2.5}$ exposure, female C57BL/6J mice received intratracheal instillations of $PM_{2.5}$ every three days for two weeks before mating, and this exposure regimen was maintained throughout gestation until delivery. We found that exposure led to behavioral deficits, including social interaction deficit and increased repetitive behaviors in both sexes, with working memory impairment specific to males. Mechanistically, $PM_{2.5}$ altered hippocampal plasticity in a sex-specific manner, increasing neural progenitors in males while reducing dendritic complexity in females. Both sexes exhibited synaptic dysfunction in the hippocampus, though there were no changes in gut microbiota profile and neuroinflammatory response. Metabolomic analysis revealed that these structural and synaptic changes were in associated with reduced hippocampal cysteine levels. Our findings suggest that hippocampal cysteine deficiency as a potential mechanism underlying maternal $PM_{2.5}$ exposure-induced hippocampal abnormality in the offspring.

Introduction

Recent epidemiological studies indicate that chronic pre- and/or postnatal exposure to particulate matter that has a diameter of less than 2.5 μm ($PM_{2.5}$) may impair neurodevelopment [5, 6]. While the etiology of neurodevelopmental disorders (NDDs) remains largely unclear, accumulating evidence suggests that environmental factors, particularly those encountered during prenatal and early postnatal development, play a critical role, either independently or through interactions with genetic susceptibility [3, 4].

Systematic reviews have highlighted the role of atmospheric PM exposure in NDDs, including cognitive decline, attention-deficit/hyperactivity disorder, and autism spectrum disorders (ASD) [7, 8]. A recent meta-analysis and systemic review support the notion that exposure to $PM_{2.5}$ during pregnancy increases risk of ASD in newborns [9]. Both prenatal and postnatal exposures to $PM_{2.5}$ are significantly associated with an increased risk of ASD [10, 11], suggesting that $PM_{2.5}$ may enhance susceptibility to the disorder. This risk is likely due to the neurotoxic components of $PM_{2.5}$ [12], such as polycyclic aromatic hydrocarbons, metals, organic matter, and elemental carbon [13], which can alter gene expression, trigger neuroinflammation, and disrupt brain development [14]. However, the impact of chronic $PM_{2.5}$ exposure on impairing neurodevelopment can't be validated in humans. Mechanisms underlying the transgenerational negative impact on neurodevelopment of maternal $PM_{2.5}$ exposure is still largely unexplored.

Evidence showing detrimental effects of $PM_{2.5}$ in offspring brain health is still in infancy. Limited study has shown that chronic exposure to $PM_{2.5}$ during pregnancy significantly decreases the number and size of cortical neurons in offspring mice [15], causing neuronal atrophy in various brain regions, including the

hippocampus [16] which is crucial for learning, memory, and emotional regulation [17, 18]. Direct $PM_{2.5}$ exposure reduces apical dendritic length in the CA1 region and decreases synaptic vesicle numbers in the hippocampus, thereby impairing synaptic plasticity [19]. Our previous study has indicated that synaptic impairment in the hippocampus could be linked to cognitive deficits observed in Fragile X mice, a commonly studied ASD model caused by single gene mutation [20]. Hippocampal abnormalities in children [21, 22] and adolescents [23, 24] with ASD have been widely reported, suggesting hippocampal dysfunction plays a significant role in neuropathology in NDDS.

Alterations in gut microbiota are increasingly recognized as contributing to gastrointestinal disturbances, social impairment, and repetitive behaviors observed in individuals with NDDs [28, 29]. Epidemiological studies indicate that $PM_{2.5}$ exposure can reduce gut microbiota diversity [30] and modify its composition during gestation [31], which may be linked to gastrointestinal diseases and neurodevelopmental outcomes. Emerging evidence suggests that changes in gut microbiota and microbiota-derived metabolites are associated with NDDs [32].

In this study, we investigated whether prolonged maternal exposure to $PM_{2.5}$ impairs behavior and hippocampal function in adult male and female offspring, and to elucidate the underlying mechanisms.

Materials and methods

Animals and experimental design

All experimental procedures were approved by the Animal Subjects Ethics Sub Committee of The Hong Kong Polytechnic University and adhered to their guidelines. C57BL/6J mice were provided with standard chow and water ad libitum and maintained in a 12-hour light-dark cycle (lights on at 9 a.m.) in the animal holding facility. To mitigate stress from social isolation, which can impact adult neurogenesis, animals were group-housed as previously described [34]. After a 2-day acclimation period, two female mice were paired with one male. Pregnancy was confirmed by the presence of seminal plugs. $PM_{2.5}$ was dissolved in artificial lung fluid (ALF) to achieve a concentration of 2.5 μg/μl, creating an ALF/$PM_{2.5}$ solution. Beginning at 5 weeks of age, female mice received $PM_{2.5}$ exposure via intratracheal instillation (30 μl) every 3 days for two weeks, after which they were housed with males for mating. Maternal $PM_{2.5}$ exposure continued until parturition. Offspring were weaned at 3 weeks of age and separated by sex into different cages on postnatal day 28 (PND 28). At 5 weeks of age, offspring underwent a series of behavioral tests under dim light conditions during the light cycle. Behavioral assessments were conducted over 7 days, with each test performed on a separate day in the following order: open field test, novel object recognition test, Y-maze test, three-chamber social interaction test, and forced swim test. To evaluate repetitive behavior, a marble burying test was conducted in a new cohort of animals after modeling. From each litter, 1–2 male and female offspring were selected for behavioral testing, one male and female offspring in each litter were taken for molecular assays.

Behavioral tests

A separate cohort of animals was designated for behavioral testing. All mice underwent a 7-day pre-handling period, followed by a two-day habituation phase in which they were exposed to the empty testing apparatus for 15 minutes each day. This pre-handling and habituation protocol is crucial for minimizing stress associated with handling and exposure to novel environments. To further reduce stress, mice were acclimated to the behavioral testing room for 2 hours prior to the commencement of tests each day. Each mouse participated in a series of behavioral assessments, with only one test administered per day to prevent confounding effects from multiple tests [35].

Three-chambered social interaction test

The three-chamber test was utilized to evaluate sociability and social novelty in mice [36]. The test consisted of three phases: habituation, sociability test, and social novelty test, and was conducted as previously described [37]. An apparatus box that was separated into three chambers was used (60 × 30 × 30 cm^3). During a 5-min habituation period, a test mouse was placed in the middle chamber of the box, and an empty wire enclosure was placed in both the first and third chambers. The test mice were permitted unrestricted access to all three chambers via the connecting doorways, allowing for free exploration throughout the apparatus. There was a 5-min interval before the next phase started. In the 10-min sociability test, a stimulus mouse was placed in the wire cage in one chamber, while the wire enclosure in the other chamber remained empty. The test mouse was then returned to the middle chamber and allowed to roam around the three chambers freely. Sociability was determined by the preference of the testing mouse for the stimulus mouse or the empty enclosure. Any direct contact or sniffing of the cage was assessed as evidence of direct exploration or touch of an enclosure or social interest in the stimulus mouse. The exploration ratio was calculated as $T_A/(T_A + T_B)$ for the mouse and $T_B/(T_A + T_B)$ for the empty enclosure. The exploration ration index was calculated as $(T_A - T_B)/(T_A + T_B)$, where T_A = time spent exploring the mouse and T_B = time spent exploring the empty enclosure. A 5-min interval was given before the final phase. In the 10-min social novelty test, a new stimulus mouse (novel mouse) was placed in the empty wire enclosure, and the test mouse was allowed to explore the chambers for 10 min. Social novelty recognition memory was evaluated based on the subject's preference for interacting with either the novel or the familiar conspecific. The exploration ratios for the familiar and novel mice were determined using the formulas $T_F/(T_F + T_N)$ and $T_N/(T_F + T_N)$, respectively, where T_F represents the time spent investigating the familiar mouse and T_N denotes the time spent with the novel mouse. Additionally, the exploration index was calculated as $(T_N - T_F)/(T_N + T_F)$ to quantify the relative preference for social novelty. The test was videotaped and analyzed by a well-trained researcher manually in a sample-blinded manner.

Novel object recognition test

A transparent plastic arena (60 × 40 × 22 cm) was used for the test. A camera was positioned directly above the box to capture the mice's movements throughout the experiment. In the adaptation period,

mice were allowed to move freely within the arena for 5 minutes to acclimate to the experimental setup. After a 5 minutes test interval in the home cage, mice were re-introduced to the arena with two identical objects (object set 1) for 10 minutes. After a 2-hour interval, one of the original objects was replaced with a novel object of similar size but different shape. Mice were then allowed to explore for 5 minutes. The time spent sniffing each object was recorded [38].The familiar exploration ratio was computed as TF/(TF + TN), and the novel exploration ratio as TN/(TF + TN), where TF and TN represent the time spent investigating the familiar and novel mice, respectively. To further quantify social novelty preference, the exploration index was calculated using the formula (TN − TF)/(TN + TF), where TF = time spent exploring the familiar mouse and TN = time spent exploring the novel mouse

Y maze

The Y-maze test, designed to assess spatial memory, was conducted in an arena consisting of three symmetrical arms made of gray plastic, each arm having the dimensions of 30 cm x 15 cm X 6 cm. These arms were arranged at 120° angles, with external spatial cues provided in the surrounding room. The test was divided into 2 phases. During phase 1, mice were permitted to explore the apparatus for 10 minutes, with one arm (designated as the novel arm) blocked off. Following a 2-hour interval, phase 2 commenced, in which the previously blocked arm was opened, allowing the mice unrestricted exploration of all arms for an additional 10 minutes. The familiar exploration ratio was calculated as $T_F/(T_F + T_N)$.The novel exploration ratio was calculated with the formula $(T_N/(T_F + T_N))$. The exploration index was calculated with the formula: $(T_N - T_F)/(T_N + T_F)$, where T_F = time spent exploring the familiar mouse and T_N = time spent exploring the novel mouse[39].

Open field test (OFT)

Each mouse was placed in the center of a square open field arena (50 × 50 × 30 cm), for 5 minutes. The total distance traveled (measured in meters) and the duration spent in the center zone (measured in seconds) were recorded and analyzed using the EthoVision XT 10 tracking system (Noldus)[37].

Forced swim test (FST)

A mouse was placed in a cylindrical container (30 cm in height and 15 cm in diameter) filled with water maintained at room temperature (24–25°C) and recorded on video for 6 minutes following established protocols [34]. An observer, blinded to the treatment conditions, assessed the time the mouse spent immobile during the final 4 minutes of the test. Immobility was defined as the absence of movement except for the minimal actions required to keep the head above water [40]. This measure was used as an indicator of depression-like behavior.

Marble burying test

Animals were housed in a standard type II cage (40 cm x 28 cm x 18 cm) with a 5 cm layer of bedding. Twenty identical black marbles were evenly distributed across the bedding. The animals were observed for a duration of one hour. A marble was considered buried when at least two-thirds of its surface area was obscured by bedding material [41].

Tissue preparation and immunohistochemistry

Offspring mice were deeply anesthetized using a cocktail of ketamine (10 mg/kg) and xylazine (4 mg/kg) and then perfused transcardially with normal saline, followed by 4% paraformaldehyde. The brains were post-fixed overnight at 4°C and subsequently immersed in 30% sucrose until they sank. Coronal sections with 30 µm thickness (1 in-6 series) were cut through the hippocampus, spanning from bregma 23.30 mm to 24.52 mm[42]. These brain sections were stored in a cryoprotectant solution consisting of 30% glycerol and 30% ethylene glycol in 1x PBS until immunostaining was performed. After washing with 0.01 M PBS, sections were incubated overnight with rabbit anti-Ki67 antibody (1:1000, Abcam), followed by biotinylated goat anti-mouse antibody (1:200, Vector Laboratories). Ki67 staining was visualized using the peroxidase method (ABC system, Vector Laboratories) and diaminobenzidine (DAB) kits (1:200, Vector Laboratories)[42]. For DCX or NeuroD staining, sections were incubated with rabbit anti-DCX (1:200, Vector Laboratories) or mouse anti-NeuroD (1:200, Vector Laboratories) antibodies, respectively, followed by the same visualization method as described above[43].

Quantification of cell proliferation and immature neurons in the hippocampus

Cell proliferation, immature neurons, and neuronal differentiation were quantified by counting Ki67, DCX, and NeuroD immunopositive cells, respectively. Total number of Ki67+, DCX+, and NeuroD+ cells present in the SGZ of either the dorsal DG (from Bregma 1.34 to 2.54), or the ventral DG (Bregma 2.54 to 3.80) sub-regions were quantified as previously performed[44]. The counts were performed using a Nikon H600L microscope (Nikon, Japan).

Sholl analysis

Immature neurons were selected based on the following criteria: (1) the neuron must be at least a tertiary immature neuron, possessing three or more dendritic branches; (2) the neuron must extend towards the molecular layer of the DG with intact dendritic branching; (3) the cell body should be located in the subgranular zone of the DG; and

(4) neurons can be selected from either the superior or inferior blade of the dentate gyrus. For each brain region, five immature neurons were traced, encompassing three dorsal and three ventral regions, resulting in a total of 30 neurons analyzed [45]. Neurons were selected under 400x magnification to measure total dendritic length and perform Sholl analysis using Neurolucida software (MicroBrightField Bioscience, VT, United States).

Golgi-Cox staining and dendritic spine counting

Golgi-Cox staining and dendritic spine counting conducted as previously performed [42, 46]. Mouse hippocampal tissues were immersed in Golgi-Cox staining solution and stored in the dark for two weeks, following the manufacturer's instructions (FD Neurotechnologies Inc., Columbia, MD). After rinsing with distilled water, the tissues were placed in 80% glacial acetic acid overnight. The tissues were subsequently sectioned into 150 μm-thick slices using a vibratome (Leica VT2000S). Five neurons per section were analyzed using Neurolucida software (MicroBrightField, USA), selected based on established criteria [47]. Only neurons situated within the dentate gyrus (DG) of the dorsal hippocampus were selected for analysis. To ensure accuracy, selected neurons were relatively isolated from neighboring stained neurons to prevent analytical interference. To minimize truncation of dendritic branches, neurons with cell bodies located near the center of the section thickness were selected for analysis. Additionally, neurons were required to be consistently and thoroughly impregnated along the entire length of all dendrites. Spine density was assessed by randomly selecting high-magnification tracings of 0.10 mm-long terminal segments from both basal and apical dendritic branches. For each neuron, three to five tertiary apical and basal dendrites, each containing at least one branch point, were chosen for analysis. The number of visible spines along these segments was counted under a microscope at 600× magnification (Axioplan, Zeiss, Oberkochen, Germany). Results were reported as the number of spines per 10 mm of dendritic length [42].

Immunostaining and quantification analysis

Antigen retrieval was performed using a citric acid heat method (pH 6.0) at 95°C for 10 minutes. Following three washes with 1x PBS for 10 minutes each, brain slices were incubated overnight with the primary antibody, rabbit anti-Iba-1 (1:1000, Abcam). Subsequently, the slices were incubated with the secondary antibody, goat anti-rabbit (1:200, Vector Laboratories). Positive cells were visualized using the VECTASTAIN ABC kit (HRP) (1:200, Vector Laboratories) and the DAB peroxidase substrate kit (1:200, Vector Laboratories). Iba-1 immunopositive cells were quantified from eight sections spanning the Bregma positions − 1.34 to -3.80 mm[48]. Sections were imaged at 200x magnification using a Nikon H600L microscope (Nikon, Japan). Quantification of inflammatory cells was carried out by counting Iba-1 immunopositive cells were counted from 8 sections across − 1.34 to -3.80 mm bregma position. The sections were scanned at 200x magnification (United States). The hippocampus was divided into the dentate gyrus (DG), cornu ammonis 1 (CA1) and cornu ammonis 3 (CA3) regions respectively using ImageJ (NIH, University of Wisconsin, United States) and Iba-1 cells in the regions were counted.

Western blot assays

Protein samples were resolved on 8% or 12% polyacrylamide gels and subsequently transferred to polyvinylidene difluoride (PVDF) membranes (Bio-Rad, Hercules, CA, USA). The membranes were blocked with 5% non-fat dry milk in TBST (Tris-buffered saline with 0.1% Tween 20) for 2 hours at room temperature. Following blocking, the membranes were washed three times with PBS at room temperature. They were then incubated overnight at 4°C with specific primary antibodies: Tubulin

(1:2000, Abcam), PSD95 (1:1000, Abcam), Synaptophysin (1:1000, Abcam), Synapsin-1 (1:1000, CST), BDNF (1:1000, Abcam), β-Actin (1:2000, Abcam), GluN2B (1:1000, Cell Signaling Technology), GluN2A (1:1000, Cell Signaling Technology), pGluN2A (1:1000, Cell Signaling Technology), pGluN2B (1:1000, Cell Signaling Technology), and GAPDH (1:10000, Bioworld, China). After three washes with TBST, the membranes were incubated for 2 hours at room temperature with horseradish peroxidase-conjugated secondary antibodies (1:10000, Proteintech). Protein bands were visualized using the ChemiDoc XRS+ Imaging System (Bio-Rad). Band intensities were quantified using Image Lab 3.0 software (Bio-Rad).

Enzyme-linked immunosorbent assay (ELISA)

ELISA procedures Following the collection of fresh tissue samples, the hippocampal region was homogenized and centrifuged at 13,000 rpm. The resulting supernatant was collected for analysis using enzyme-linked immunosorbent assay (ELISA)[42]. ELISA procedures were conducted according to the protocols provided in the commercial kits. Three commercial kits were utilized: High Mobility Group Box 1 protein (HMGB1), tumor necrosis factor-alpha (TNF-α), and Matrix Metallopeptidase 9 (MMP-9), all from CUSABIO (Houston). The supernatant was added to the ELISA plate and incubated for 2 hours. This was followed by sequential incubations with a biotin conjugated antibody for 1 hour and an avidin-conjugated antibody for another hour. Subsequently, the 3,3',5,5'-Tetramethylbenzidine substrate was added and allowed to react for 15 minutes. Finally, a stop solution was added, and the absorbance was immediately measured at 450 nm and 570 nm.

Quantification of amino acids in the hippocampus

The hippocampus was homogenized in a 0.9% NaCl solution at a ratio of 1:3 (w/v). The resulting homogenate was extracted with two volumes of pre-chilled acetonitrile and then centrifuged at 17,000 g for 10 minutes. The supernatant was derivatized using the Kairos Amino Acid Kit (Waters, Milford, MA, USA) and quantified via ultra-high-performance liquid chromatography coupled with triple quadrupole mass spectrometry (UHPLC-QqQ-MS/MS). Amino acid analysis was conducted on an Agilent 1290 Infinity II UHPLC system paired with an Agilent 6460 Triple Quadrupole Mass Spectrometer equipped with an electrospray ionization (ESI) source (Agilent Technologies Inc., Santa Clara, CA, USA), following a modified version of the method by Lo et al[49]. Chromatographic separation was achieved using a Waters CORTECS UPLC C18 column (2.1 x 150 mm, 1.6 μm) with a Waters CORTECS C18 VanGuard Pre-column (2.1 x 150 mm, 1.6 μm). The binary mobile phase consisted of (A) water with 0.1% formic acid and (B) acetonitrile with 0.1% formic acid. Gradient elution was performed at a flow rate of 0.3 mL/min, starting at 2% B from 0 to 1.5 minutes, increasing to 9% at 4 minutes, 11% at 5 minutes, 13% at 18 minutes, and 95% from 18.5 to 20.5 minutes, before returning to initial conditions in 0.1 minutes and equilibrating for 4.4 minutes prior to the next injection. The column temperature was maintained at 55°C, and the autosampler was kept at room temperature. The injection volume was 2 μL.

Electrophysiological field recording

Acute hippocampal slice preparation

Following deep anesthesia with isoflurane, the mice were promptly decapitated. The brains were immediately immersed for one minute in ice-cold normal artificial cerebrospinal fluid (nACSF), composed of 125 mM NaCl, 2.5 mM KCl, 1.25 mM NaHPO4, 25 mM NaHCO3, 2 mM CaCl2, and 1.3 mM MgCl2, with a pH of 7.3. This solution was oxygenated with a 95% O2/5% CO2 mixture, as described in our previous protocol [50]. Transverse brain slices, 300 μm thick, were prepared using a fully automated vibratome (VT1200 S, Leica Biosystems Inc., IL, USA). These slices were then transferred to separate compartments of an incubation chamber filled with normal ACSF, continuously supplied with carbogen, and allowed to recover at 35°C for at least one hour prior to recording.

Field recording

The hippocampal slice was placed on a MED Probe equipped with 64 microelectrodes (P515A, Alpha MED Scientific Inc., Osaka, Japan). The electrodes were precisely positioned within the middle molecular layer of the suprapyramidal blade to stimulate granule neurons, following a previously established protocol [51] and guided by a light microscope. The slices were continuously perfused with nACSF at 28°C at a flow rate of 2 ml/min. Field excitatory postsynaptic potentials (fEPSPs) were recorded using amplifiers (MED-A64MD1 and MED-A64HE1S, Alpha MED Scientific Inc., Osaka, Japan) and acquired with Mobius software (Alpha MED Scientific Inc.) interfaced to a computer. The stimulus intensity was set between 25–35 μA for each slice to achieve 40–50% of the maximum response slope, while avoiding population spikes. After a 20-minute stabilization period with single-pulse stimulations at 15-second intervals, high-frequency stimulation (HFS) was applied. This involved four trains of 50 pulses at 100 Hz with a 30-second intertrain interval, in the presence of picrotoxin (100 μM), a GABAA receptor antagonist, to induce LTP. Input-output (I/O) experiments were conducted to measure responses with increasing stimulation intensity, using 9 trains with a 10-second intertrain interval and increasing intensity of 10 μA. Additionally, presynaptic release probability was assessed using a paired pulse (PP) protocol in nACSF, consisting of 5 sets of two pulses with a 20 ms interval and a 20-second interval between paired stimuli.

Gut microbiota analysis

DNA extraction

DNA was extracted from 36 fecal samples using the TIANamp Stool DNA Kit (DP328-02, China) according to the manufacturer's instructions. The extracted DNA samples were stored at − 80°C until sequencing. For the polymerase chain reaction (PCR), 30 ng of qualified DNA template was combined with 16S rRNA fusion primers. PCR products were purified using Agencourt AMPure XP beads, dissolved in Elution Buffer, and labeled to complete library construction. The size and concentration of the libraries were assessed using an Agilent 2100 Bioanalyzer. Qualified libraries were then sequenced on the HiSeq platform based on their insert size.

PCR amplification

The library was prepared using the 2× Phanta Max Master Mix (VAZYME, China) polymerase. The V3V4 variable region of bacterial 16S rDNA was amplified using forward and reverse degenerate primers, 338F

(ACTCCTACGGGAGGCAGCAG) and 806R (GGACTACHVGGGTWTCTAAT). PCR enrichment was conducted in a 50 μL reaction volume containing 30 ng of template DNA and fusion PCR primers. The PCR cycling conditions were as follows: an initial denaturation at 95°C for 3 minutes, followed by 30 cycles of 95°C for 15 seconds, 56°C for 15 seconds, and 72°C for 45 seconds, with a final extension at 72°C for 5 minutes. PCR products were purified using DNA magnetic beads (BGI, LB00V60). Subsequently, the final double-stranded library products were denatured to produce single-stranded library products. A circularization reaction was then performed to obtain single-stranded circular DNA products, with any remaining single-stranded linear DNA being digested and removed. The final single-stranded circular library was amplified using phi29 and rolling circle amplification (RCA) to generate DNA nanoballs (DNBs), which contain multiple copies of the initial single-stranded library molecule. The DNBs were loaded onto a patterned nanoarray, and sequencing reads of 300 base pairs in length were generated using the DNBSEQ-G400 platform (BGI, China).

Processing of reads and data analysis

Intestinal sample raw reads were processed using the DADA2 plugin within the QIIME2 platform (version 2024.5) to perform denoising and generate amplicon sequence variants (ASVs). Taxonomic assignment of ASVs was conducted using the SILVA 138 reference database, with a similarity threshold of 99%. On average, each sample yielded 44,698 ± 2,061 high-quality reads. Rarefaction was conducted at a depth of 40,800 sequences, corresponding to the sample with the fewest sequences, utilizing the q2-diversity plugin in QIIME2. Alpha diversity, based on this rarefaction depth, was evaluated using the Shannon index, calculated via the q2-diversity plugin. Principal coordinate analysis (PCoA) based on Bray-Curtis dissimilarity was conducted using the "vegan" package (version 2.6-4) in R. Compositional differences were assessed through permutational multivariate analysis of variance (PERMANOVA) and analysis of similarities (ANOSIM), both implemented in the "vegan" package. Statistical differences between two groups were assessed using the nonparametric Mann-Whitney U test, whereas comparisons among more than two groups were performed using the Kruskal-Wallis test. Both tests were conducted using the "stats" package (version 4.2.2) in R. A p-value of less than 0.05 was considered statistically significant.

Statistical analysis

All statistical analyses were conducted using GraphPad Prism 9.0 (GraphPad Software, San Diego, CA, USA). Two-way analysis of variance (ANOVA) was conducted, with $PM_{2.5}$ exposure and gender as between-subject factors. Post hoc analyses were performed using Tukey's or Fisher's tests, as appropriate. For comparisons between two groups, a two-tailed Student's t-test was employed when appropriate. Raw amino acid data were processed using MassHunter Quantitative Analysis software (Agilent Technologies, Santa Clara, CA, USA). For the diversity and composition of intestinal microbiota, statistical differences between two groups were determined using the nonparametric Mann-Whitney U test, while differences among more than two groups were assessed using the Kruskal-Wallis test. A p-value of less than 0.05 was considered statistically significant. Values are expressed as mean ± standard error of the mean (SEM).

Results

Maternal exposure to $PM_{2.5}$ induced behavioral deficits in adult offspring

In the sociability test, all offspring mice spent significantly more time sniffing the unfamiliar stimulus mouse compared to the empty chamber (Fig. 2A1, Students' T-test: males-control: $t_5 = 11.57$, $P < 0.0001$; females-control: $t_4 = 12.29$, $P = 0.0003$; males-$PM_{2.5}$: $t_5 = 59.63$, $P < 0.0001$; females-$PM_{2.5}$: $t_5 = 19.84$, $P < 0.0001$), indicating a strong preference for the chamber containing the mouse. A two-way ANOVA of the social preference index revealed a significant effect of treatment (Fig. 2A2: $F (1, 19) = 47.23$, $P < 0.0001$) but no significant effect of sex ($F (1, 19) = 0.01152$, $P = 0.9157$) and interaction ($F (1, 19) = 2.869$, $P = 0.1067$). Post-hoc test revealed that maternal $PM_{2.5}$ increased exploration index in both male and female offspring (males-control vs males-$PM_{2.5}$: $P < 0.01$, females-control vs females-$PM_{2.5}$ $P < 0.0001$), suggesting maternal $PM_{2.5}$ affected sociability in both male and female offspring.

In the social novelty test, control male and female offspring spent significantly more time sniffing the novel stimulus mouse (S2) compared to the familiar stimulus mouse (S1) (Fig. 2B1, Students' T-test: males-control: $t5 = 3.786$, $P < 0.05$; females-control: $t4 = 3.639$, $P < 0.05$), suggesting intact social novelty recognition memory. Male offspring (Fig. 2B1, males-$PM_{2.5}$: $t5 = 5.215$, $P < 0.001$) but not female offspring (females-$PM_{2.5}$: $t5 = 0.6012$, $P = 0.5739$) from dams with maternal $PM_{2.5}$ exposure showed significantly higher exploration ratio to the stimulus mouse. A two-way ANOVA of the social novelty index revealed a significant effect of treatment (Fig. 2A2: 471 $F (1, 19) = 5.654$, $P = 0.0281$) but no significant effect of sex ($F (1, 19) = 2.896$, $P = 0.1051$) and interaction ($F (1, 19) = 0.01797$, $P = 0.8948$). Post- hoc analysis showed no significant difference in exploration index among groups but a decreased trend, suggesting maternal $PM_{2.5}$ had a tendency to affect social novelty in both male and female offspring (males-control vs males-$PM_{2.5}$: $P = 0.3886$; females-control vs females-$PM_{2.5}$: $P = 0.3339$).

To assess repetitive behavior using the marble burying test, there was a significant effect of treatment (Fig. 2C: $F (1, 22) = 13.71$, $P = 0.0012$) but no significant effect of sex ($F (1, 22) = 0.3608$, $P = 0.5542$) and interaction ($F (1, 22) = 1.661e-005$, $P = 0.9968$). Post-hoc analysis revealed no statistically significant differences in the number of buried marbles between groups (males-control vs males-$PM_{2.5}$: $P = 0.0697$; females control vs females-$PM_{2.5}$: $P = 0.0689$). However, the data indicate a strong trend toward an increase in buried marbles in the $PM_{2.5}$-exposed groups, suggesting increased repetitive behavior in offspring.

Maternal exposure to $PM_{2.5}$ impaired working memory in male offspring

All control offspring demonstrated a significantly greater preference for the novel object compared to the familiar object (Fig. 3A1, Students' T-test: males-control: $t_5 = 11.06$, $P < 0.001$; females-control: $t_4 = 4.063$,

P < 0.05), whereas male and female offspring with $PM_{2.5}$-exposed dams showed no difference in exploration ratio (males-$PM_{2.5}$: t_5 = 1.014, P = 0.357; females-$PM_{2.5}$: t_5 = 0.3964, P = 0.7082). In the exploration index, a two-way ANOVA revealed a main effect of $PM_{2.5}$ (Fig. 3A2, F (1, 19) = 15.17, P = 0.0010) and effect of sex (F (1, 19) = 6.412, P = 0.0203), though no significant interaction (F (1, 19) = 1.504, P = 0.235). Notably, maternal $PM_{2.5}$ significantly reduced exploration index in male offspring, indicating impaired working memory compared to control male offspring (Fig. 3A2, Tukey post hoc test: P = 0.0074 males: control vs. $PM_{2.5}$). In contrast, $PM_{2.5}$ exposure did not significantly affect working memory in female offspring compared to controls (Fig. 3A2, P = 0.2849 females: control vs. $PM_{2.5}$).

Spatial memory was evaluated using the Y-maze test. Control male and female offspring showed significantly more exploration of the novel arm (Fig. 3B1, Students' T-test: males-control: t4 = 6.862, P < 0.01; females-control: t4 = 3.492, P < 0.05). $PM_{2.5}$ exposed male offspring showed significant difference in exploration between novel and familiar arms but maternal $PM_{2.5}$-exposed female offspring did not exhibit significant differences in exploration (males-control: t6 = 2.749, P < 0.05; females-control: t6 = 1.223, P = 0.2673). Two-way ANOVA of the exploration index showed significant gender (Fig. 3B2, F (1, 22) = 5.5, P = 0.0291) and treatment effects (F (1, 22) = 10, P = 0.0043), but not interaction effect (F (1, 22) = 0.52, P = 0.4771). There were no significant differences in exploration index (Fig. 3B2, Tukey post hoc test: males: control vs. males: $PM_{2.5}$: P = 0.328) and female offspring (females: control vs. females:$PM_{2.5}$: P = 0.0515).

The open field test assessed locomotor activity (Fig. 3C1) and anxiety-like behavior (Fig. 3C2). Two-way ANOVA showed no interaction effects for distance traveled (interaction: F(1, 19) = 0.2172, P = 0.6465; gender factor: F (1, 19) = 0.09725, P = 0.7586; $PM_{2.5}$ factor: F (1, 19) = 0.005082, P = 0.9439), and time spent in the center (interaction: F (1, 19) = 0.5773, P = 0.4567; gender factor F (1, 19) = 0.05048, P = 517 0.8246; $PM_{2.5}$ Factor F (1, 19) = 2.431, P = 0.1355). Tukey post hoc test showed that no significant changes were observed in distance traveled (males: control vs. males: $PM_{2.5}$: P = 0.9794, females: control vs. females: $PM_{2.5}$: P = 0.9927) or time spent in the center (males: control vs. males: $PM_{2.5}$: P = 0.9371, females: control vs. females: $PM_{2.5}$: P = 0.401) between control and $PM_{2.5}$-exposed groups. Two-way ANOVA showed no interaction effects for immobility in the forced swimming test (interaction factor F (1, 19) = 2.070, P = 0.1665; gender factor F (1, 19) = 0.02094, P = 0.8865; $PM_{2.5}$ factor F (1, 19) = 0.01981, P = 0.8896), indicating no significant difference in depression-like behavior in offspring.

Maternal exposure to $PM_{2.5}$ enhanced hippocampal cell proliferation and neuronal differentiation in male offspring

We investigated the effects of maternal exposure to $PM_{2.5}$ on hippocampal neurogenesis in offspring, focusing on cell proliferation and neuronal differentiation. Neurogenesis was evaluated by quantifying cell proliferation (Ki67+), the population of immature neurons (DCX+), and neuronal differentiation (NeuroD+).

Our findings indicate that maternal exposure to $PM_{2.5}$ significantly increased the number of Ki67 + cells in the dorsal and ventral DG of male offspring, as demonstrated by a main effect of $PM_{2.5}$ treatment ($F(1, 19) = 14.72$, $P = 0.0011$), though no significant interaction ($F(1, 19) = 2.377$, $P = 0.1396$) and sex effect ($F(1, 19) = 0.4581$, $P = 0.5067$). Similarly, the analysis of the ventral DG revealed a significant main effect of $PM_{2.5}$ ($F(1, 19) = 9.003$, $P = 0.0074$) and a significant interaction effect ($F(1, 19) = 4.394$, $P = 0.0497$), although no main effect of sex ($F(1, 19) = 0.7991$, $P = 0.3825$). Post hoc tests confirmed that maternal $PM_{2.5}$ exposure increased Ki67 + cell proliferation in both dorsal and ventral DG of male offspring compared to control group ($P < 0.01$), while no significant differences were observed in females (dorsal: $P = 0.4098$; ventral: $P = 0.9228$). Furthermore, maternal $PM_{2.5}$ exposure significantly increased the number of NeuroD+ cells in the dorsal DG, indicating a significant treatment effect ($F(1, 19) = 99$, $P < 0.0001$), but without a significant sex effect ($F(1, 19) = 0.0049$, $P = 0.9447$) or interaction ($F(1, 19) = 0.94$, $P = 0.3444$). However, maternal $PM_{2.5}$ exposure did not affect the number of NeuroD+ cells in the ventral DG following maternal $PM_{2.5}$ exposure, with no treatment effect ($F(1, 19) = 3.723$, $P = 0.0688$), sex effect ($F(1, 19) = 0.5598$, $P = 0.4635$) or interaction ($F(1, 19) = 0.4415$, $P = 0.5144$). Post hoc tests confirmed that maternal $PM_{2.5}$ exposure highly increased NeuroD+ cells in both male and female offspring compared to control group in dorsal DG ($P < 0.0001$), while no significant effects were observed in the ventral DG for either sex (males: $P = 0.7964$; females: $P = 0.3075$ compared to control counterpart).

The two-way ANOVA analysis showed that maternal exposure to $PM_{2.5}$ did not significantly affect the number of DCX+ cells in the dorsal DG for either sex (main effect of treatment: $F(1, 18) = 0.7912$, $P = 0.3855$; main effect of sex: $F(1, 18) = 0.2672$, $P = 0.6115$; interaction: $F(1, 18) = 0.1956$, $P = 0.6636$). Post hoc tests revealed no significant increase in DCX+ cells in the dorsal DG of male offspring ($P = 0.7831$ $PM_{2.5}$ vs. control) and female offspring ($P = 0.9887$ $PM_{2.5}$ vs. control). Similarly, $PM_{2.5}$ exposure did not affect the ventral DG (treatment: ($F(1, 19) = 9.003$, $P = 0.0074$); sex effect ($F(1, 19) = 0.7991$ $P = 0.3825$; interaction effect ($F(1, 19) = 0.94$, $P = 0.3444$). Post-hoc analyses showed no significant differences in the number of DCX+ cells in the ventral DG between the $PM_{2.5}$-exposed and control groups for male offspring ($P = 0.9812$) and female offspring ($P > 0.9999$).

In conclusion, our study indicates sex-specific effects of maternal $PM_{2.5}$ exposure on hippocampal neurogenesis, with significant increases in cell proliferation and neuronal differentiation observed in male offspring.

Maternal exposure to $PM_{2.5}$ reduced dendritic branch length of hippocampal immature neurons in female offspring

We next examined whether maternal $PM_{2.5}$ exposure induced retardation on dendritic development, morphological analysis of immature neurons (DCX+ cell was performed using Sholl analysis (Fig. 5A). A two-way ANOVA revealed a main effect of treatment (Fig. 5B: $F(1, 95) = 10.29$, $P = 0.0018$) and highly sex-specific effect ($F(1, 95) = 5.105$, $P = 0.0261$) on total dendritic length, but no interaction effect ($F(1,$

95) = 0.7734, P = 0.3814) was observed. Post-hoc analysis indicated a significant reduction in total dendritic length in female offspring exposed to $PM_{2.5}$ compared to controls (P < 0.05), whereas no significant difference was found in male offspring (P = 0.3623 vs. control male offspring). There was no significant difference in dendritic length in offspring (Fig. 5C: main effect of treatment: F (1, 20) = 2.480, P = 0.1310; main effect of sex: F (1, 20) = 1.834, P = 0.1908; interaction: F (1, 20) = 0.6017, P = 0.4470).

Golgi-Cox staining (Fig. 5D) demonstrated that maternal exposure to $PM_{2.5}$ did not affect the density of dendritic spines in the hippocampal DG region in either male or female offspring (Fig. 5E: main effect of treatment: F (1, 22) = 0.42, P = 0.5241; main effect of sex: F(1, 22) = 1.4, P = 0.2457; interaction: F(1, 22) = 0.47, P = 0.4999).

Maternal exposure to PM impaired hippocampal synaptic plasticity in both male and female offspring

Field recording revealed that maternal exposure to $PM_{2.5}$ resulted in a significant reduction in LTP in both male and female pups (Fig. 6A: main effect of treatment: F (1, 316) = 91.37, P < 0.0001; main effect of sex: F (1, 316) = 5.459, P = 0.0201; interaction: F (1, 316) = 3.382, P = 0.0669). Tukey post hoc test confirmed that a significant reduction in LTP of male offspring (P < 0.0001 $PM_{2.5}$ vs. control) and female offspring (P < 0.0001 $PM_{2.5}$ vs. control). This reduction was evidenced by a significant decrease in the average fEPSP slope change compared to control mice (Fig. 6B: main effect of treatment: F (1, 44) = 44.58, P < 0.0001; main effect of sex: F (1, 44) = 0.01991, P = 0.8884; interaction: F (1, 44) = 0.4213, P = 0.5197). Post hoc tests revealed a significant decrease in the average fESP slope change of male offspring (P < 0.0001; main effect of sex: F (18, 312) = 0.1169, P > 604 0.9999; interaction: F (3, 312) = 0.4959, P = 0.6854), suggesting that basal synaptic transmission remains intact.

To evaluate short-term plasticity using a paired-pulse conditioning stimulation protocol, there was no significant difference (Fig. 6D; main effect of treatment: F (1, 44) = 1.871, P = 0.1783; main effect of sex: F (1, 44) = 0.1751, P = 0.6777; interaction: F (1, 44) = 0.1280, P = 0.7222).Collectively, these results suggest that chronic maternal exposure to $PM_{2.5}$ reduced hippocampal LTP formation in offspring, impairing synaptic plasticity in the DG region of the hippocampus.

Maternal exposure to $PM_{2.5}$ reduced synaptic proteins in offspring

We next examined changes of synaptic proteins in the hippocampal tissues (Fig. 7A). Figure 7A- Two-way ANOVA revealed a main sex-specific effect (F (1, 20) = 8.423, P = 0.0088) and interaction effect (F (1, 20) = 8.423, P = 0.0088), but not a treatment-specific effect (F (1, 20) = 0.6247, P = 0.4386), on hippocampal brain-derived neurotrophic factor (BDNF) levels (Fig. 7B). Post-hoc analysis indicated that maternal $PM_{2.5}$ exposure did not significantly affect BDNF levels in either sex compared to controls

(males: P = 0.4598; females: P = 0.9379). $PM_{2.5}$ exposure did not significantly alter the levels of synaptophysin (SYN) (Fig. 7C: interaction: F (1, 20) = 0.5700, P = 0.4591; gender: F (1, 20) = 0.5700, P = 0.4591; $PM_{2.5}$: F (1, 20) = 0.003697, P = 0.9521) and PSD-95 proteins (Fig. 7D: PSD-95, interaction: F (1, 20) = 0.5700, P = 0.4591; gender: F (1, 20) = 0.5700, P = 0.4591; $PM_{2.5}$: F (1, 20) = 0.003697, P = 0.9521) in the hippocampi of offspring mice. $PM_{2.5}$ treatment did not affect GluN2A protein levels (Fig. 7E gender effect (F (1, 20) = 1.054, P = 0.3169) and interaction effect (F (1, 20) = 1.054, P = 0.3169). However, there was a main treatment effect (Fig. 7F. (F (1, 20) = 24.40, P < 0.0001), but not sex-specific effect (F (1, 20) = 0.01762, P = 0.8957) and interaction effect (F (1, 20) = 0.01762, P = 0.8957) on hippocampal GluN2B levels. Post-hoc tests revealed that maternal $PM_{2.5}$ exposure reduced GluN2B protein expression in the hippocampi of both male and female offspring (males: P < 0.01 $PM_{2.5}$ vs. control; females: P < 0.01 $PM_{2.5}$ vs. control), suggesting impaired LTP formation could be linked to reduction in GluN2B subunit of the NMDA receptors.

Metabolomic analysis of amino acid levels in the hippocampus of offspring

Amino acids play crucial roles in NDDs associated with ASD [52, 53]. To investigate the effect of maternal exposure to $PM_{2.5}$ on hippocampal amino acid levels in both mothers and offspring mice, we measured the concentrations of twenty standard amino acids in the hippocampus (Fig. 8A). Targeted metabolomics revealed a significant decrease in the concentration of glutamic acid in the $PM_{2.5}$-exposed mothers (PMO group: 386 ± 11 μM) than in the control mothers (CMO group: 422 ± 7 μM) (Fig. 8B: p < 0.05). A two-way ANOVA revealed no significant differences in glutamic acid levels in the offspring mice (Fig. 8B: interaction: F (1, 17) = 0.3579, P = 0.5575; gender: F (1, 17) = 0.01324, P = 0.9097; $PM_{2.5}$: F (1, 17) = 0.3050, P = 0.5880). Offspring mice displayed significant decrease in cysteine levels. A two-way ANOVA indicated a significant treatment-specific effect on hippocampal cysteine levels, but no sex-specific effect was found (main effect of treatment: F (1, 19) = 52.75, P < 0.0001; main effect of sex: F (1, 19) = 2.329, P = 0.1434; interaction: F (1, 19) = 2.040, P = 0.1694). Specifically, both female and male offspring with dams exposed to $PM_{2.5}$ exhibited significantly lower cysteine concentrations compared to those in the control groups with Tukey's post-hoc test (Fig. 8C: males: P < 0.01, females: P < 0.001).

Maternal exposure to $PM_{2.5}$ did not induce neuroinflammation in the 654 hippocampus of offspring

Our study aims to investigate whether maternal exposure to $PM_{2.5}$ induces NDD-like behaviors in offspring and whether these behaviors are associated with a neuroinflammatory response. We assessed neuroinflammation by examining the number of ionized calcium-binding adapter molecule 1 (IBA-1) positive microglial cells in the hippocampus. Two-way ANOVA revealed no significant inflammatory response in the hippocampal subregions in the DG (Fig. 9B: interaction: F (1, 20) = 0.8710, P = 0.3618; gender: F (1, 20) = 0.1625, P = 0.6911; $PM_{2.5}$: F (1, 20) = 0.9950, P = 0.3304) and CA3 region (Fig. 9D: interaction: (F (1, 20) = 0.5972, P = 0.4487; gender: F (1, 20) = 0.06823, P = 0.7966; $PM_{2.5}$: F (1, 20) =

1.184, P = 0.2896). A two-way ANOVA showed a main treatment-specific effect (F (1, 20) = 6.203, P = 0.0217), but not sex-specific effect (F (1, 20) = 1.672, P = 0.2107) and interaction effect (F (1, 20) = 0.3840, P = 0.5424) on inflammatory response in the hippocampal subregions in the CA1 region. Post hoc analysis confirmed no significant changes in the number of IBA-1 positive cells in the DG (males: P > 0.9999, females: P = 0.5344), CA1 (males: P = 0.5597, females: P = 0.1576), and CA3 (males: P = 0.996, females: P = 0.564).

Additionally, there were no significant changes in the levels of HMGB1, TNF-α, and MMP-9 proteins (Fig. 9E-G). The ANOVA results showed no significant effects for HMGB1 (Fig. 9E: interaction: (F (1, 20) = 1.802, P = 0.1945; gender: F (1, 20) = 0.4713, P = 0.5003; $PM_{2.5}$: F (1, 20) = 0.5959, P = 0.4492) and MMP-9 levels (Fig. 9G: interaction: (F (1, 20) = 0.3252, P = 0.5749; gender: F (1, 20) = 0.04604, P = 0.8323; $PM_{2.5}$: F (1, 20) = 1.137, P = 0.2989). A two-way ANOVA showed a main sex-specific effect (F (1, 16) = 4.483, P = 0.0503), but not treatment-specific effect (F (1, 20) = 1.672, P = 0.2107) and interaction effect (F (1, 16) = 0.02486, P = 0.8767) on TNF-α level.

Furthermore, post hoc tests indicated no significant differences in hippocampal levels of HMGB1 (males: P > 0.9999, females: P = 0.5344), TNF-α (males: P = 0.4017, females: P = 0.5256), and MMP-9 (males: P = 0.6595, females: P = 0.9847) across all groups. These findings suggest that maternal $PM_{2.5}$ exposure does not induce a detectable neuroinflammatory response in the hippocampus of offspring.

Intestinal microbiota in male offspring with decreased relative abundance of Bacteroidaceae family

In the analysis of alpha-diversity, the Shannon index revealed that $PM_{2.5}$-exposed groups had significantly lower diversity compared to healthy groups (P = 0.020, Fig. 10A). However, no significant differences were observed in the Shannon index for male offspring (P = 0.240 vs. control male offspring) and female offspring (P = 0.589 vs. Control female offspring) when exposed to $PM_{2.5}$. A marginally significant difference

was noted in female mother groups between $PM_{2.5}$-exposed and healthy groups (P = 0.065, Fig. 10A). Regarding beta-diversity, a main treatment-specific effect was identified, but no gender-specific effect was observed (Fig. 10B, PERMANOVA: Interaction: R^2 = 0.170, P = 0.269; $PM_{2.5}$: R^2 = 0.031, P = 0.290; Gender: R^2 = 0.102, P 696 = 0.006). The ANOSIM test indicated a significant difference in the intestinal bacterial communities of female mothers between $PM_{2.5}$-exposed and healthy groups (R = 0.233, 698 P = 0.024). The top 10 most abundant bacterial genera across all samples were analyzed to identify functionally important taxa affected by $PM_{2.5}$ exposure (Fig. 10C). The dominant genus was Muribaculaceae, with no significant differences observed in these genera upon $PM_{2.5}$ exposure. Further comparisons of the most abundant bacterial classes (Fig. 10D) and families (Fig. 10E) revealed a significantly lower relative abundance of the classes Campylobacteria (P = 0.026 vs. control female mother) and Saccharimonadia (P = 0.026 vs. control female mother) in female mothers exposed to $PM_{2.5}$ compared to healthy groups (Fig. 10D). Additionally, a significantly lower relative abundance of the

family Bacteroidaceae (P = 0.015 vs. control male offspring) was found in $PM_{2.5}$-treated male offspring compared to healthy groups (Fig. 10E).

Discussion

We found that offspring from mother exposure to $PM_{2.5}$ displayed behavioral abnormalities and hippocampal dysfunction with a gender effect. Both male and female offspring showed some behavioral abnormalities in association with male offspring exhibiting more proliferating progenitor cells and immature neurons in the hippocampus, while females showing reduced dendritic length of immature neurons. Both sexes displayed significant impairments in LTP formation and synaptic GluN2B protein expression, and a significant decrease in cysteine levels in the hippocampus. These changes are independent of neuroinflammatory responses and changes in gut microbiota profile. Our findings suggest that maternal $PM_{2.5}$ exposure may contribute to NDD-like behavioral abnormality in offspring, with hippocampal dysfunction. These changes could be linked to reduced cysteine levels in the hippocampus.

Previous epidemiological studies have shown that prenatal and/or postnatal exposure to $PM_{2.5}$ increases the likelihood of offspring developing NDDs [54–56], with some studies suggesting that this exposure could potentially double the risk of NDD development [57]. In rodent models, direct exposure to $PM_{2.5}$ in young rats has been associated with autistic-like behaviors [58]. Contrary to the reduced sociability typically observed in classic ASD models, our findings showed that offspring exposed to maternal PM2.5 exhibited enhanced social preference in the sociability phase. However, in the social novelty phase, a female-specific deficit in recognizing novel social stimuli emerged, reminiscent of the social cognitive impairments seen in NDDs. Our results provided evidence showing the link between maternal $PM_{2.5}$ exposure and behavioral deficits in adult offspring that assemble some NDD-like behaviors.

Defects in neuronal maturation have been observed in multiple regions associated with NDD, suggesting dysregulation in adult neurogenesis, neuronal migration, and/or maturation [59]. Our findings indicate increased proliferating cells and mature neurons in the hippocampus, with no change in the number of immature neurons or spine density following exposure, but a reduction in the total dendritic length of immature neurons in female offspring. In contrast, Wang et al. reported that maternal exposure to $PM_{2.5}$ decreases neurogenesis rates [60]. This could be due to the fact that exposure to $PM_{2.5}$ at different developmental stages may yield different effect on neuronal development and function [61]. In our study, mice were 42 days old, primarily reflecting adult neurogenesis, whereas Wang's study involved mice at 14 days old, a period of active developmental stages. Similarly, Juliandi et al. found that prenatal exposure to valproic acid in an autism model of mice led to cognitive impairments postnatally, potentially due to premature enhancement of embryonic neurogenesis [62]. This premature enhancement may deplete the neural progenitor cell (NPC) pool, subsequently inhibiting adult hippocampal neurogenesis. In ferret pups, exposure to VPA resulted in disrupted social behaviors and

promoted the proliferation of neural progenitor cells in the DG, introducing additional NPCs into the DG granule cell layer [63]. This observation aligns with our research findings.

In the cellular culture analysis of reprogrammed fibroblasts, induced pluripotent stem cells, neural progenitor cells, and neurons derived from individuals with NDDs exhibited increased cell proliferation [64]. Similarly, three-dimensional neural cultures from induced pluripotent stem cells of individuals with NDDs demonstrated upregulation of genes associated with cell proliferation and neuronal differentiation [65]. Watanabe et al. found that developmental exposure to risk factors in autistic rats primarily affects interneurons, which later impacts the proliferation of neural progenitor cells in the subgranular zone, leading to an increased number of granule cell layer neurons in the rat hippocampus [66]. Other studies, through the analysis of neuronal ultrastructure, have found that exposure to $PM_{2.5}$ during pregnancy leads to an increase in synaptic clefts, thinning of postsynaptic density, shortening of synaptic active zones, as well as swelling of mitochondrial matrix, partial blurring of mitochondrial cristae, and mitochondrial vacuolation in the hippocampal neurons of mouse offspring[67, 68]. These findings align with our results, which demonstrate an increase in neuronal differentiation. However, further investigation is needed to identify the specific types of neurons involved. Although the number of immature neurons remained relatively unchanged, we observed a notable reduction in total dendritic length in female offspring. Collectively, these studies, [69] along with our data, suggest that dysregulation of neural progenitor cell proliferation and delayed neuronal maturation occurred in the hippocampus with a gender specific effect. Changes of hippocampal structural plasticity may partly contribute to core behavioral deficits associated with NDDs. Our research provides unique insights into the significant structural changes in hippocampal neurons resulting from maternal exposure to $PM_{2.5}$.

Synaptic plasticity is regulated by various mechanisms, including changes in receptor numbers, neurotransmitter release, and synaptic site localization. Maternal $PM_{2.5}$ exposure may alter dendritic branching, dendritic spine density, and morphology, potentially disrupt these processes and impair synaptic transmission in the offspring's brain. $PM_{2.5}$ exposure reduced cell viability, increased apoptosis, and synaptic damage in primary cultured hippocampal neurons [14, 69]. N-Methyl-D-Aspartate receptor (NMDAR)-dependent synaptic plasticity is a key mediator of hippocampus-dependent learning and memory processes [70, 71]. Alterations in signaling of NMDARs containing the GluN2B subunit can inhibit dendritic spine density and impair learning capabilities [72]. In this study, we observed a reduction in LTP in the offspring, suggesting that maternal $PM_{2.5}$ exposure diminishes hippocampal long-term synaptic plasticity. Western blotting revealed a significant decrease in GluN2B expression in the hippocampus of $PM_{2.5}$-exposed offspring compared to controls. Previous studies have shown that the absence of GluN2B in the hippocampus impairs dendritic spine density and hippocampal-mediated learning and memory[73, 74], underscoring the critical role of GluN2B in modulating synaptic plasticity. Further investigation into the potential mechanisms linking GluN2B and hippocampal synaptic plasticity in offspring exposed to $PM_{2.5}$ is warranted.

Numerous studies have identified a link between maternal inflammation during early pregnancy and an increased risk of NDDs [75]. Our results showed no significant changes in the levels of HMGB1, TNF-α, MMP-9 proteins, or in the number of Iba-1 positive microglial cells in the hippocampus. These findings are consistent with postmortem studies of the hippocampal region by Vargas et al., which also reported no significant inflammation [76]. Another study found no pronounced inflammation in the hippocampus but observed abnormally small and densely distributed hippocampal neurons with reduced complexity and dendritic arbor length [77]. These observations suggest that hippocampal inflammation may not be the necessary mechanism underlying $PM_{2.5}$-induced NDDs during pregnancy. Instead, alterations in neuronal maturation and differentiation might contribute to behavioral deficits. Some studies have reported increased inflammation only in high-dose $PM_{2.5}$ groups [78]. In contrast, our study used lower doses, which may explain the differences in findings. Further research is needed to determine the specific $PM_{2.5}$ dose and duration of exposure required to trigger neuroinflammation.

Synaptic plasticity and memory function in the brain are primarily driven by NMDAR, which require the binding of glutamate and the co-agonist D-serine at the glycine site. Cysteine also plays a crucial role in hippocampal synaptic plasticity, influencing synaptic transmission [79, 80], neuronal connectivity [81], and the regulation of the intracellular environment [82], thereby affecting learning and memory. In this study, metabolomic analysis revealed that maternal exposure to $PM_{2.5}$ results in decreased glutamate levels in the maternal body and reduced cysteine levels in the offspring's hippocampal tissue. Research indicates that melatonin treatment significantly increased cysteine-rich protein 1 levels, contributing to dendritic branching in mouse hippocampal neurons[83]. Neuronal uptake of cysteine via excitatory amino acid carriers can mitigate ischemia-induced neuronal death by promoting glutathione synthesis in the hippocampus of ischemic animal models [83]. Furthermore, administration of L-cysteine (L-Cys) has been shown to improve behavioral, biochemical, neurochemical, and redox status in the central nervous system[84]. Prenatal supplementation with the antioxidant N-acetyl cysteine (NAC) offers protective benefits for fetal neurodevelopment against the adverse effects of prenatal restraint stress and maternal high-fat diet [85]. Early supplementation with antioxidants such as NAC or L-Cys may represent a promising therapeutic strategy for addressing NDDs. Our results discovered deficiency of cysteine in the hippocampus of offspring displaying hippocampal atrophy and behavioral deficit, suggesting the critical role of cysteine in the impact of $PM_{2.5}$ on hippocampal function.

The maternal microbiome also plays a critical role in offspring’s neurodevelopment [85], possibly because maternal gut microbiota affects the availability of essential metabolites required for fetal development [33]. Clinical studies have demonstrated that changes of gut microbiota found in children with NDDs are also presented in their mothers [86], and gut microbiota shared in children and their mothers is related to developmental disability and social behavioral deficits [87]. Findings from animal research provide further support for the link between microbiota and NDDs in clinical studies. Previous studies have shown that alterations in the gut microbiota can lead to long-term enhancements in adult neurogenesis [88] and synaptic transmission[89]. Gut microbiota can influence brain function and behavior by producing various metabolites, such as short-chain fatty acids and neurotransmitter

precursors [90]. Our findings revealed that $PM_{2.5}$ exposure significantly decreased abundance of the Bacteroidaceae family only in male offspring. These findings suggest that maternal gut microbiota potentially influenced by environmental exposures such as $PM_{2.5}$ may contribute to offspring neurodevelopmental outcomes in a sex-specific manner, possibly through alterations in microbiota composition and associated metabolite production.

Conclusion

Our study provides evidence that maternal exposure to $PM_{2.5}$ significantly impacts hippocampal function of offspring with a gender effect, resulting in behavioral deficit in offspring. These effects could be linked to structural and functional alterations in the hippocampus, including disrupted synaptic plasticity and neuronal dendric development. Specifically, $PM_{2.5}$ exposure leads to notable reductions in cysteine levels in the hippocampus, which may contribute to hippocampal impairment induced by maternal $PM_{2.5}$ exposure. These findings suggest the connection between maternal $PM_{2.5}$ exposure, reduction of cysteine levels and alterations in hippocampal plasticity, providing evidence showing the possible impacts of $PM_{2.5}$ on inducing behavioral abnormalities in offspring's brain development.

Declarations

Conflict of interests

All authors declare no conflict of interest.

Funding

This work was funded by Research Grants Council (RGC) General Research Fund (15104620) and Mental Health Research Center (MHRC) from Hong Kong Polytechnic University.

Authors contribution

Conceptualization, Y.Z. A. and S.Y.Y; Methodology, A. T.C. J.M.R. Y.Y. D.Z. S.D. P.K.H. and S.Y.Y; Validation, A. Y.Z.T.C. J.M.R. Y.Y. D.Z. S.D. P.K.H. H.A. J.Y. D.A.F. and S.Y.Y; Formal Analysis, Y.Z. T.C. H.A. J.M.R. Y.Y. S.D. P.K.H. and S.Y.Y; Data Curation, Y.Z. and S.Y.Y; Investigation, D.A.F. Y.Y.H. C.C.H.C. H.G. and S.Y.Y; Resources, S.Y.Y. H.G. D.Z. P.K.H.; Software, Y.Z. A. Y.Y. D.Z. S.D. P.K.H. J.M.R. H.A.; Writing—Original Draft, Y.Z. and S.Y.Y; Writing—Review & Editing, Y.Z. A.Y.Y. S.D. and S.Y.Y; Visualization, Y.Z. Y.Y. S.D. and S.Y.Y; Supervision, D.A.F. Y.Y.H. C.C.H.C. H.G. and S.Y.Y; Project Administration, S.Y.Y; Funding Acquisition, S.Y.Y.

Acknowledgments

We thank the equipment and technical support by University Research Facility in Behavioral and Systems Neuroscience, The Hong Kong Polytechnic University.

References

1. Baio J, Wiggins L, Christensen DL, Maenner MJ, Daniels J, Warren Z, Kurzius-Spencer M, Zahorodny W, Robinson Rosenberg C, White T *et al*: Prevalence of Autism Spectrum Disorder Among Children Aged 8 Years - Autism and Developmental Disabilities Monitoring Network, 11 Sites, United States, 2014. *MMWR Surveill Summ* 2018, 67(6).
2. Sun X, Allison C, Wei L, Matthews FE, Auyeung B, Wu YY, Griffiths S, Zhang J, Baron-Cohen S, Brayne C: Autism prevalence in China is comparable to Western prevalence. *Mol Autism* 2019, 10:7.
3. Lyall K, Croen L, Daniels J, Fallin MD, Ladd-Acosta C, Lee BK, Park BY, Snyder NW, Schendel D, Volk H *et al*: The Changing Epidemiology of Autism Spectrum Disorders. *Annu Rev Public Health* 2016, 38.
4. Modabbernia A, Velthorst E, Reichenberg A: Environmental risk factors for autism: an evidence-based review of systematic reviews and meta-analyses. *Mol Autism* 2017, 8:13.
5. Raz R, Roberts AL, Lyall K, Hart JE, Just AC, Laden F, Weisskopf MG: Autism spectrum disorder and particulate matter air pollution before, during, and after pregnancy: a nested case-control analysis within the Nurses' Health Study II Cohort. *Environ Health Perspect* 2014, 123(3):264–270.
6. Flores-Pajot M-C, Ofner M, Do MT, Lavigne E, Villeneuve PJ: Childhood autism spectrum disorders and exposure to nitrogen dioxide, and particulate matter air pollution: A review and meta-analysis. *Environ Res* 2016, 151:763–776.
7. Ruiz-Sobremazas D, Rodulfo-Cárdenas R, Ruiz-Coca M, Morales-Navas M, Teresa Colomina M, López-Granero C, Sánchez-Santed F, Perez-Fernandez C: Uncovering the link between air pollution and neurodevelopmental alterations during pregnancy and early life exposure: A systematic review. *Neurosci Biobehav Rev* 2023, 152:105314.
8. Lyall K, Schmidt RJ, Hertz-Picciotto I: Maternal lifestyle and environmental risk factors for autism spectrum disorders. *Int J Epidemiol* 2014, 43(2):443–464.
9. Dutheil F, Comptour A, Morlon R, Mermillod M, Pereira B, Baker JS, Charkhabi M, Clinchamps M, Bourdel N: Autism spectrum disorder and air pollution: A systematic review and meta-analysis. *Environ Pollut* 2021, 278:116856.
10. Lin H-H, Jung C-R, Lin C-Y, Chang Y-C, Hsieh C-Y, Hsu P-C, Chuang B-R, Hwang B-F: Prenatal and postnatal exposure to heavy metals in PM2.5 and autism spectrum disorder. *Environ Res* 2023, 237(Pt 1):116874.
11. Rahman MM, Shu Y-H, Chow T, Lurmann FW, Yu X, Martinez MP, Carter SA, Eckel SP, Chen J-C, Chen Z *et al*: Prenatal Exposure to Air Pollution and Autism Spectrum Disorder: Sensitive Windows of Exposure and Sex Differences. *Environ Health Perspect* 2022, 130(1):17008.

12. Kumar RK, Shadie AM, Bucknall MP, Rutlidge H, Garthwaite L, Herbert C, Halliburton B, Parsons KS, Wark PAB: Differential injurious effects of ambient and traffic-derived particulate matter on airway epithelial cells. *Respirology* 2014, 20(1):73–79.
13. Allen JL, Liu X, Pelkowski S, Palmer B, Conrad K, Oberdörster G, Weston D, Mayer-Pröschel M, Cory-Slechta DA: Early postnatal exposure to ultrafine particulate matter air pollution: persistent ventriculomegaly, neurochemical disruption, and glial activation preferentially in male mice. *Environ Health Perspect* 2014, 122(9):939–945.
14. Ahadullah, Yau S-Y, Lu H-X, Lee TMC, Guo H, Chan CCH: PM2.5 as a potential risk factor for autism spectrum disorder: Its possible link to neuroinflammation, oxidative stress and changes in gene expression. *Neurosci Biobehav Rev* 2021, 128:534–548.
15. Zheng X, Wang X, Wang T, Zhang H, Wu H, Zhang C, Yu L, Guan Y: Gestational Exposure to Particulate Matter 2.5 (PM2.5) Leads to Spatial Memory Dysfunction and Neurodevelopmental Impairment in Hippocampus of Mice Offspring. *Front Neurosci* 2019, 12:1000.
16. Power MC, Lamichhane AP, Liao D, Xu X, Jack CR, Gottesman RF, Mosley T, Stewart JD, Yanosky JD, Whitsel EA: The Association of Long-Term Exposure to Particulate Matter Air Pollution with Brain MRI Findings: The ARIC Study. *Environ Health Perspect* 2018, 126(2):027009.
17. Rossi CC, Van de Water J, Rogers SJ, Amaral DG: Detection of plasma autoantibodies to brain tissue in young children with and without autism spectrum disorders. *Brain Behav Immun* 2011, 25(6):1123–1135.
18. Raymond GV, Bauman ML, Kemper TL: Hippocampus in autism: a Golgi analysis. *Acta Neuropathol* 1996, 91(1):117–119.
19. Greco CM, Navarro CS, Hunsaker MR, Maezawa I, Shuler JF, Tassone F, Delany M, Au JW, Berman RF, Jin L-W *et al*: Neuropathologic features in the hippocampus and cerebellum of three older men with fragile X syndrome. *Mol Autism* 2011, 2(1):2.
20. Yau S-Y, Bettio L, Chiu J, Chiu C, Christie BR: Fragile-X Syndrome Is Associated With NMDA Receptor Hypofunction and Reduced Dendritic Complexity in Mature Dentate Granule Cells. *Frontiers In Molecular Neuroscience* 2018, 11:495.
21. Barnea-Goraly N, Frazier TW, Piacenza L, Minshew NJ, Keshavan MS, Reiss AL, Hardan AY: A preliminary longitudinal volumetric MRI study of amygdala and hippocampal volumes in autism. *Progress In Neuro-psychopharmacology & Biological Psychiatry* 2014, 48:124–128.
22. Schumann CM, Hamstra J, Goodlin-Jones BL, Lotspeich LJ, Kwon H, Buonocore MH, Lammers CR, Reiss AL, Amaral DG: The amygdala is enlarged in children but not adolescents with autism; the hippocampus is enlarged at all ages. *J Neurosci* 2004, 24(28):6392–6401.
23. Groen W, Teluij M, Buitelaar J, Tendolkar I: Amygdala and hippocampus enlargement during adolescence in autism. *J Am Acad Child Adolesc Psychiatry* 2010, 49(6):552–560.
24. Aylward EH, Minshew NJ, Goldstein G, Honeycutt NA, Augustine AM, Yates KO, Barta PE, Pearlson GD: MRI volumes of amygdala and hippocampus in non-mentally retarded autistic adolescents and adults. *Neurology* 1999, 53(9):2145–2150.

25. McBean GJ: Cysteine, Glutathione, and Thiol Redox Balance in Astrocytes. *Antioxidants (Basel)* 2017, 6(3).
26. Janáky R, Varga V, Hermann A, Saransaari P, Oja SS: Mechanisms of L-cysteine neurotoxicity. *Neurochemical Research* 2000, 25(9–10):1397–1405.
27. Kulak A, Steullet P, Cabungcal J-H, Werge T, Ingason A, Cuenod M, Do KQ: Redox dysregulation in the pathophysiology of schizophrenia and bipolar disorder: insights from animal models. *Antioxid Redox Signal* 2012, 18(12):1428–1443.
28. Roussin L, Prince N, Perez-Pardo P, Kraneveld AD, Rabot S, Naudon L: Role of the Gut Microbiota in the Pathophysiology of Autism Spectrum Disorder: Clinical and Preclinical Evidence. *Microorganisms* 2020, 8(9).
29. Oh D, Cheon K-A: Alteration of Gut Microbiota in Autism Spectrum Disorder: An Overview. *Soa Chongsonyon Chongsin Uihak* 2020, 31(3):131–145.
30. Ran Z, An Y, Zhou J, Yang J, Zhang Y, Yang J, Wang L, Li X, Lu D, Zhong J *et al*: Subchronic exposure to concentrated ambient PM2.5 perturbs gut and lung microbiota as well as metabolic profiles in mice. *Environ Pollut* 2020, 272:115987.
31. Liu W, Zhou Y, Yong L, Qin Y, Yu L, Li R, Chen Y, Xu Y: Effects of PM2.5 exposure during gestation on maternal gut microbiota and pregnancy outcomes. *Chemosphere* 2020, 247:125879.
32. Yap IKS, Angley M, Veselkov KA, Holmes E, Lindon JC, Nicholson JK: Urinary metabolic phenotyping differentiates children with autism from their unaffected siblings and age-matched controls. *Journal of Proteome Research* 2010, 9(6):2996–3004.
33. Vuong HE, Pronovost GN, Williams DW, Coley EJL, Siegler EL, Qiu A, Kazantsev M, Wilson CJ, Rendon T, Hsiao EY: The maternal microbiome modulates fetal neurodevelopment in mice. *Nature* 2020, 586(7828):281–286.
34. Yau SY, Li A, Hoo RLC, Ching YP, Christie BR, Lee TMC, Xu A, So K-F: Physical exercise-induced hippocampal neurogenesis and antidepressant effects are mediated by the adipocyte hormone adiponectin. *Proc Natl Acad Sci U S A* 2014, 111(44):15810–15815.
35. Yau SY, Bostrom CA, Chiu J, Fontaine CJ, Sawchuk S, Meconi A, Wortman RC, Truesdell E, Truesdell A, Chiu C *et al*: Impaired bidirectional NMDA receptor dependent synaptic plasticity in the dentate gyrus of adult female Fmr1 heterozygous knockout mice. *Neurobiol Dis* 2016, 96:261–270.
36. Yau SY, Chiu C, Vetrici M, Christie BR: Chronic minocycline treatment improves social recognition memory in adult male Fmr1 knockout mice. *Behavioural Brain Research* 2016, 312:77–83.
37. Yau S-Y, Yip YSL, Formolo DA, He S, Lee THY, Wen C, Hryciw DH: Chronic consumption of a high linoleic acid diet during pregnancy, lactation and post-weaning period increases depression-like behavior in male, but not female offspring. *Behavioural Brain Research* 2022, 416:113538.
38. Block ML, Calderón-Garcidueñas L: Air pollution: mechanisms of neuroinflammation and CNS disease. *Trends Neurosci* 2009, 32(9):506–516.
39. Alexander JF, Seua AV, Arroyo LD, Ray PR, Wangzhou A, Heiβ-Lückemann L, Schedlowski M, Price TJ, Kavelaars A, Heijnen CJ: Nasal administration of mitochondria reverses chemotherapy-induced

cognitive deficits. *Theranostics* 2021, 11(7):3109–3130.

40. Yau S-Y, Lee TH-Y, Formolo DA, Lee W-L, Li LC-K, Siu PM, Chan CCH: Effects of Maternal Voluntary Wheel Running During Pregnancy on Adult Hippocampal Neurogenesis, Temporal Order Memory, and Depression-Like Behavior in Adult Female and Male Offspring. *Front Neurosci* 2019, 13:470.
41. Wiebe S, Nagpal A, Truong VT, Park J, Skalecka A, He AJ, Gamache K, Khoutorsky A, Gantois I, Sonenberg N: Inhibitory interneurons mediate autism-associated behaviors via 4E-BP2. *Proc Natl Acad Sci U S A* 2019, 116(36):18060–18067.
42. Yau S-Y, Lau BW-M, Tong J-B, Wong R, Ching Y-P, Qiu G, Tang S-W, Lee TMC, So K-F: Hippocampal neurogenesis and dendritic plasticity support running-improved spatial learning and depression-like behaviour in stressed rats. *PloS One* 2011, 6(9):e24263.
43. Lau BW-M, Yau S-Y, Lee TMC, Ching Y-P, Tang S-W, So K-F: Effect of corticosterone and paroxetine on masculine mating behavior: possible involvement of neurogenesis. *J Sex Med* 2011, 8(5):1390–1403.
44. Yau S-Y, Lee TH-Y, Li A, Xu A, So K-F: Adiponectin Mediates Running-Restored Hippocampal Neurogenesis in Streptozotocin-Induced Type 1 Diabetes in Mice. *Front Neurosci* 2018, 12:679.
45. Ramirez-Rodriguez G, Ortíz-López L, Domínguez-Alonso A, Benítez-King GA, Kempermann G: Chronic treatment with melatonin stimulates dendrite maturation and complexity in adult hippocampal neurogenesis of mice. *J Pineal Res* 2011, 50(1):29–37.
46. Lee TH, Ahadullah, Christie BR, Lin K, Siu PM-F, Zhang L, Yuan T-F, Komal P, Xu A, So K-F *et al*: Chronic AdipoRon Treatment Mimics the Effects of Physical Exercise on Restoring Hippocampal Neuroplasticity in Diabetic Mice. *Mol Neurobiol* 2021, 58(9):4666–4681.
47. Woolley CS, Gould E, McEwen BS: Exposure to excess glucocorticoids alters dendritic morphology of adult hippocampal pyramidal neurons. *Brain Res* 1990, 531(1–2):225–231.
48. Chao M-W, Yang C-H, Lin P-T, Yang Y-H, Chuang Y-C, Chung M-C, Tseng C-Y: Exposure to PM2.5 causes genetic changes in fetal rat cerebral cortex and hippocampus. *Environ Toxicol* 2017, 32(4):1412–1425.
49. Lo EKK, Wang X, Lee P-K, Wong H-C, Lee JC-Y, Gómez-Gallego C, Zhao D, El-Nezami H, Li J: Mechanistic insights into zearalenone-accelerated colorectal cancer in mice using integrative multi-omics approaches. *Comput Struct Biotechnol J* 2023, 21:1785–1796.
50. Yau SY, Bostrom C, Chiu J, Fontaine C, Sawchuk S, Meconi A, Wortman R, Truesdell E, Truesdell A, Chiu C: Impaired bidirectional NMDA receptor dependent synaptic plasticity in the dentate gyrus of adult female Fmr1 heterozygous knockout mice. *Neurobiology of disease* 2016, 96:261–270.
51. Lee TH, Ahadullah, Christie BR, Lin K, Siu PM-f, Zhang L, Yuan T-f, Komal P, Xu A, So K-f: Chronic AdipoRon treatment mimics the effects of physical exercise on restoring hippocampal neuroplasticity in diabetic mice. *Molecular neurobiology* 2021, 58(9):4666–4681.
52. Fung LK, Flores RE, Gu M, Sun KL, James D, Schuck RK, Jo B, Park JH, Lee BC, Jung JH *et al*: Thalamic and prefrontal GABA concentrations but not GABAA receptor densities are altered in high-functioning adults with autism spectrum disorder. *Mol Psychiatry* 2021, 26(5):1634–1646.

53. Drenthen GS, Barendse EM, Aldenkamp AP, van Veenendaal TM, Puts NAJ, Edden RAE, Zinger S, Thoonen G, Hendriks MPH, Kessels RPC *et al*: Altered neurotransmitter metabolism in adolescents with high-functioning autism. *Psychiatry Res Neuroimaging* 2016, 256:44–49.
54. Becerra TA, Wilhelm M, Olsen J, Cockburn M, Ritz B: Ambient air pollution and autism in Los Angeles county, California. *Environ Health Perspect* 2013, 121(3):380–386.
55. Raz R, Roberts AL, Lyall K, Hart JE, Just AC, Laden F, Weisskopf MG: Autism spectrum disorder and particulate matter air pollution before, during, and after pregnancy: a nested case-control analysis within the Nurses' Health Study II Cohort. *Environ Health Perspect* 2015, 123(3):264–270.
56. Talbott EO, Arena VC, Rager JR, Clougherty JE, Michanowicz DR, Sharma RK, Stacy SL: Fine particulate matter and the risk of autism spectrum disorder. *Environ Res* 2015, 140:414–420.
57. Volk HE, Lurmann F, Penfold B, Hertz-Picciotto I, McConnell R: Traffic-related air pollution, particulate matter, and autism. *JAMA Psychiatry* 2013, 70(1):71–77.
58. Zhang M, Liu W, Zhou Y, Li Y, Qin Y, Xu Y: Neurodevelopmental toxicity induced by maternal PM2.5 exposure and protective effects of quercetin and Vitamin C. *Chemosphere* 2018, 213:182–196.
59. Wegiel J, Kuchna I, Nowicki K, Imaki H, Wegiel J, Marchi E, Ma SY, Chauhan A, Chauhan V, Bobrowicz TW *et al*: The neuropathology of autism: defects of neurogenesis and neuronal migration, and dysplastic changes. *Acta Neuropathol* 2010, 119(6):755–770.
60. Zheng X, Wang X, Wang T, Zhang H, Wu H, Zhang C, Yu L, Guan Y: Gestational Exposure to Particulate Matter 2.5 (PM2.5) Leads to Spatial Memory Dysfunction and Neurodevelopmental Impairment in Hippocampus of Mice Offspring. *Front Neurosci* 2018, 12:1000.
61. Xia Y-Y, de Seymour JV, Yang X-J, Zhou L-W, Liu Y, Yang Y, Beck KL, Conlon CA, Mansell T, Novakovic B *et al*: Hair and cord blood element levels and their relationship with air pollution, dietary intake, gestational diabetes mellitus, and infant neurodevelopment. *Clin Nutr* 2023, 42(10):1875–1888.
62. Juliandi B, Tanemura K, Igarashi K, Tominaga T, Furukawa Y, Otsuka M, Moriyama N, Ikegami D, Abematsu M, Sanosaka T *et al*: Reduced Adult Hippocampal Neurogenesis and Cognitive Impairments following Prenatal Treatment of the Antiepileptic Drug Valproic Acid. *Stem Cell Reports* 2015, 5(6).
63. Sawada K, Kamiya S, Aoki I: The Proliferation of Dentate Gyrus Progenitors in the Ferret Hippocampus by Neonatal Exposure to Valproic Acid. *Front Neurosci* 2021, 15:736313.
64. Gormanns P, Mueller NS, Ditzen C, Wolf S, Holsboer F, Turck CW: Phenome-transcriptome correlation unravels anxiety and depression related pathways. *Journal of Psychiatric Research* 2011, 45(7):973–979.
65. Goyer RA: Results of lead research: prenatal exposure and neurological consequences. *Environ Health Perspect* 1996, 104(10):1050–1054.
66. Watanabe Y, Murakami T, Kawashima M, Hasegawa-Baba Y, Mizukami S, Imatanaka N, Akahori Y, Yoshida T, Shibutani M: Maternal Exposure to Valproic Acid Primarily Targets Interneurons Followed by Late Effects on Neurogenesis in the Hippocampal Dentate Gyrus in Rat Offspring. *Neurotoxicity Research* 2017, 31(1):46–62.

67. Fortoul TI: Health Effects of Metals in Particulate Matter. In., edn.: IntechOpen; 2015.
68. Guo Y-P, Commons KG: Serotonin neuron abnormalities in the BTBR mouse model of autism. *Autism Res* 2017, 10(1):66–77.
69. Costa LG, Chang Y-C, Cole TB: Developmental Neurotoxicity of Traffic-Related Air Pollution: Focus on Autism. *Curr Environ Health Rep* 2017, 4(2):156–165.
70. Gray JA, Shi Y, Usui H, During MJ, Sakimura K, Nicoll RA: Distinct modes of AMPA receptor suppression at developing synapses by GluN2A and GluN2B: single-cell NMDA receptor subunit deletion in vivo. *Neuron* 2011, 71(6):1085–1101.
71. Murphy JA, Stein IS, Lau CG, Peixoto RT, Aman TK, Kaneko N, Aromolaran K, Saulnier JL, Popescu GK, Sabatini BL *et al*: Phosphorylation of Ser1166 on GluN2B by PKA is critical to synaptic NMDA receptor function and Ca2 + signaling in spines. *J Neurosci* 2014, 34(3):869–879.
72. Raybuck JD, Hargus NJ, Thayer SA: A GluN2B-Selective NMDAR Antagonist Reverses Synapse Loss and Cognitive Impairment Produced by the HIV-1 Protein Tat. *J Neurosci* 2017, 37(33):7837–7847.
73. Brigman JL, Wright T, Talani G, Prasad-Mulcare S, Jinde S, Seabold GK, Mathur P, Davis MI, Bock R, Gustin RM *et al*: Loss of GluN2B-containing NMDA receptors in CA1 hippocampus and cortex impairs long-term depression, reduces dendritic spine density, and disrupts learning. *J Neurosci* 2010, 30(13):4590–4600.
74. Wang X, Xie J, Tan L, Lu Y, Shen N, Li J, Hu H, Li H, Li X, Cheng L: N6-methyladenosine-modified circRIMS2 mediates synaptic and memory impairments by activating GluN2B ubiquitination in Alzheimer's disease. *Translational Neurodegeneration* 2023, 12(1):53.
75. Hogan MK, Kovalycsik T, Sun Q, Rajagopalan S, Nelson RJ: Combined effects of exposure to dim light at night and fine particulate matter on C3H/HeNHsd mice. *Behavioural Brain Research* 2015, 294:81–88.
76. Vargas DL, Nascimbene C, Krishnan C, Zimmerman AW, Pardo CA: Neuroglial activation and neuroinflammation in the brain of patients with autism. *Ann Neurol* 2005, 57(1):67–81.
77. Kemper TL, Bauman M: Neuropathology of infantile autism. *Journal of Neuropathology and Experimental Neurology* 1998, 57(7):645–652.
78. Zhang T, Zheng X, Wang X, Zhao H, Wang T, Zhang H, Li W, Shen H, Yu L: Maternal Exposure to PM2.5 during Pregnancy Induces Impaired Development of Cerebral Cortex in Mice Offspring. *Int J Mol Sci* 2018, 19(1).
79. Pu L, Kopec AM, Boyle HD, Carew TJ: A novel cysteine-rich neurotrophic factor in Aplysia facilitates growth, MAPK activation, and long-term synaptic facilitation. *Learn Mem* 2014, 21(4):215–222.
80. Zareba-Koziol M, Bartkowiak-Kaczmarek A, Figiel I, Krzystyniak A, Wojtowicz T, Bijata M, Wlodarczyk J: Stress-induced Changes in the S-palmitoylation and S-nitrosylation of Synaptic Proteins. *Mol Cell Proteomics* 2019, 18(10):1916–1938.
81. Park M, Baek I-J, Kim H, Woo DK, Park Y-J, Shim S: CCN3 overexpression inhibits growth of callosal projections via upregulation of RAB25. *Biochem Biophys Res Commun* 2015, 461(3):456–462.

82. Mannan A, Germon ZP, Chamberlain J, Sillar JR, Nixon B, Dun MD: Reactive Oxygen Species in Acute Lymphoblastic Leukaemia: Reducing Radicals to Refine Responses. *Antioxidants (Basel)* 2021, 10(10).
83. Ang MJ, Kang S, Moon C: Melatonin alters neuronal architecture and increases cysteine-rich protein 1 signaling in the male mouse hippocampus. *Journal of Neuroscience Research* 2020, 98(11):2333–2348.
84. Samad N, Rafeeque M, Imran I: Free-L-Cysteine improves corticosterone-induced behavioral deficits, oxidative stress and neurotransmission in rats. *Metabolic Brain Disease* 2023, 38(3):983–997.
85. Jašarević E, Bale TL: Prenatal and postnatal contributions of the maternal microbiome on offspring programming. *Front Neuroendocrinol* 2019, 55:100797.
86. Li N, Yang J, Zhang J, Liang C, Wang Y, Chen B, Zhao C, Wang J, Zhang G, Zhao D *et al*: Correlation of Gut Microbiome Between ASD Children and Mothers and Potential Biomarkers for Risk Assessment. *Genomics Proteomics Bioinformatics* 2019, 17(1):26–38.
87. Chen Y, Fang H, Li C, Wu G, Xu T, Yang X, Zhao L, Ke X, Zhang C: Gut Bacteria Shared by Children and Their Mothers Associate with Developmental Level and Social Deficits in Autism Spectrum Disorder. *mSphere* 2020, 5(6).
88. Ogbonnaya ES, Clarke G, Shanahan F, Dinan TG, Cryan JF, O'Leary OF: Adult Hippocampal Neurogenesis Is Regulated by the Microbiome. *Biological Psychiatry* 2015, 78(4):e7-e9.
89. Darch HT, Collins MK, O'Riordan KJ, Cryan JF: Microbial memories: Sex-dependent impact of the gut microbiome on hippocampal plasticity. *The European Journal of Neuroscience* 2021, 54(4):5235–5244.
90. Foster JA, McVey Neufeld K-A: Gut-brain axis: how the microbiome influences anxiety and depression. *Trends Neurosci* 2013, 36(5):305–312.

Figures

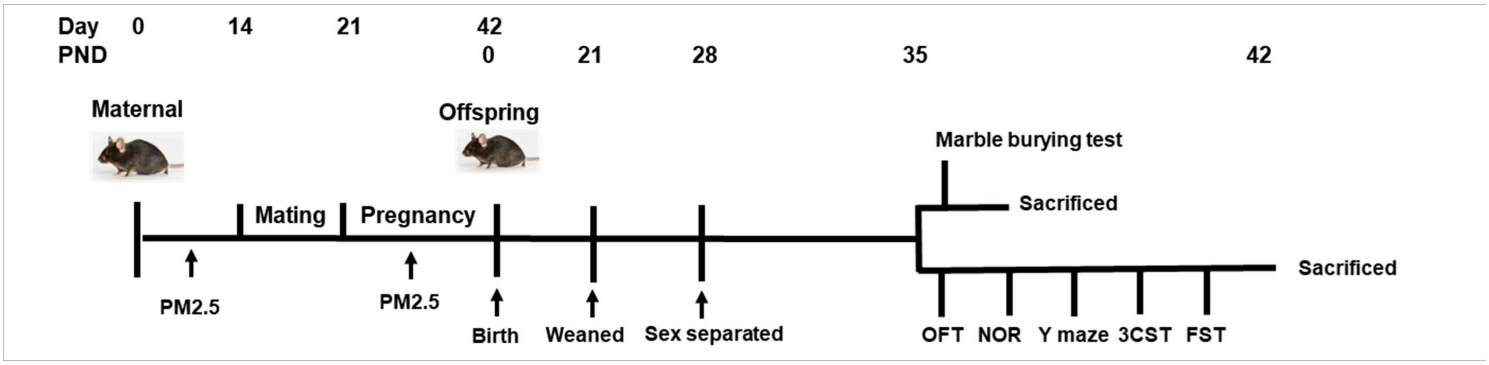


Figure 1

Treatment Timeline. Female mice, aged 5 weeks, were exposed to $PM_{2.5}$ via intratracheal instillation every three days for two weeks. Following this exposure period, the females were housed with male mice

for mating. Maternal exposure to $PM_{2.5}$ continued until parturition. Offspring were weaned at 3 weeks of age and separated by sex on postnatal day 28 (PND 28). At 5 weeks of age, the offspring underwent a series of behavioral tests. OFT: open field test; NOR: novel object recognition test; Y maze; 3CST: three-chamber social interaction test; FST: forced swim test; Marble burying test.

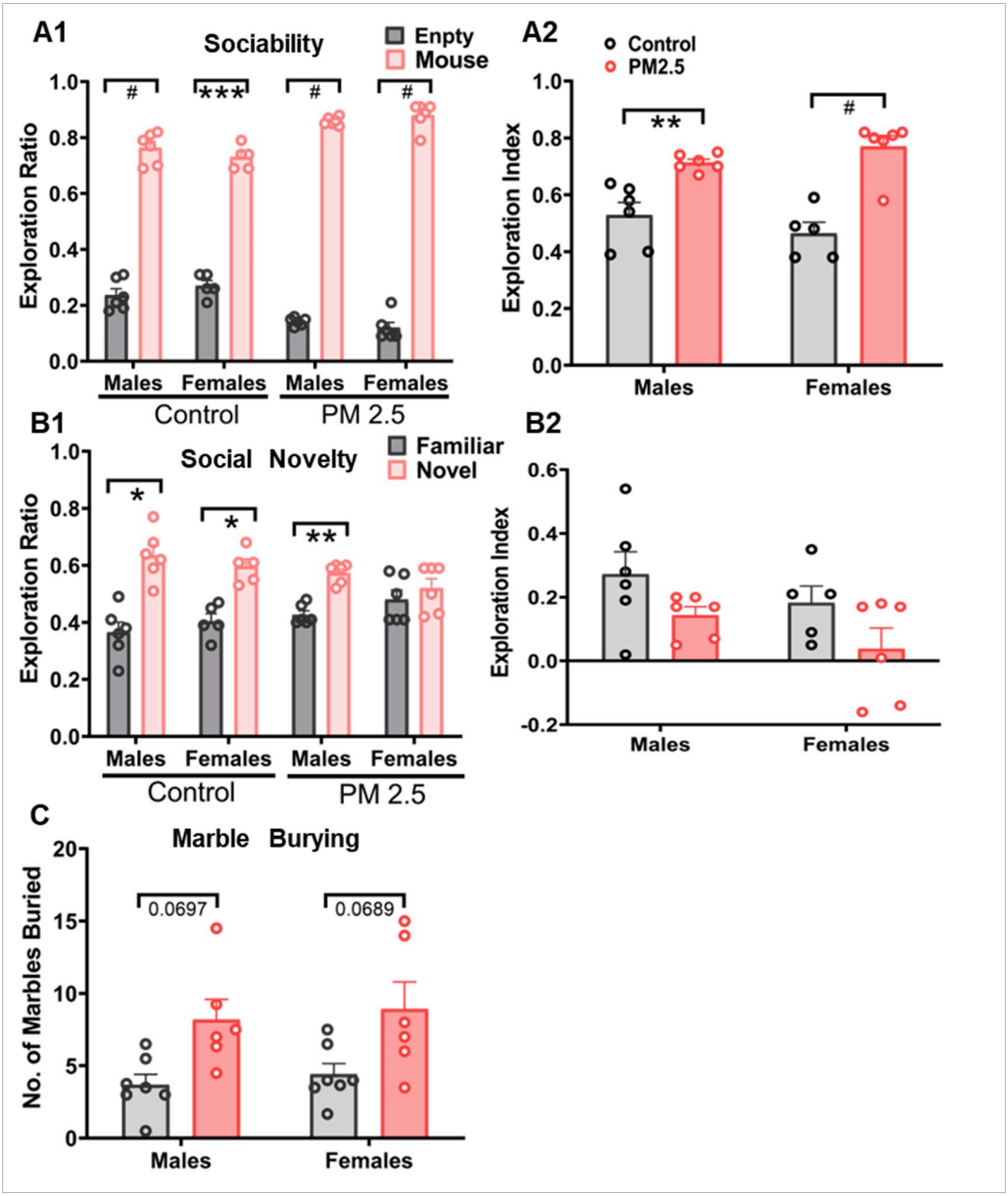


Figure 2

Maternal $PM_{2.5}$ exposure reduced social novelty and increased repetitive behaviors in adult offspring mice. (A-B) The three-chamber social interaction test was used to assess sociability and preference for social novelty. (A1) the exploration ratio indicates sociability (paired t-test: **P < 0.001; #P < 0.0001vs empty enclosure). (B1) the exploration ratio for preference for social novelty (paired t-test: *P < 0.05; **P < 0.01 vs familiar mouse). (A2 and B2) the exploration index (males: **P < 0.01; females: #P < 0.0001) identified using a two-way ANOVA with Tukey's post-hoc test for multiple comparisons. (C) the marble burying test, which measures repetitive behavior, as determined by a two-way ANOVA with Tukey's post-hoc test. n = 5–7 mice per group.

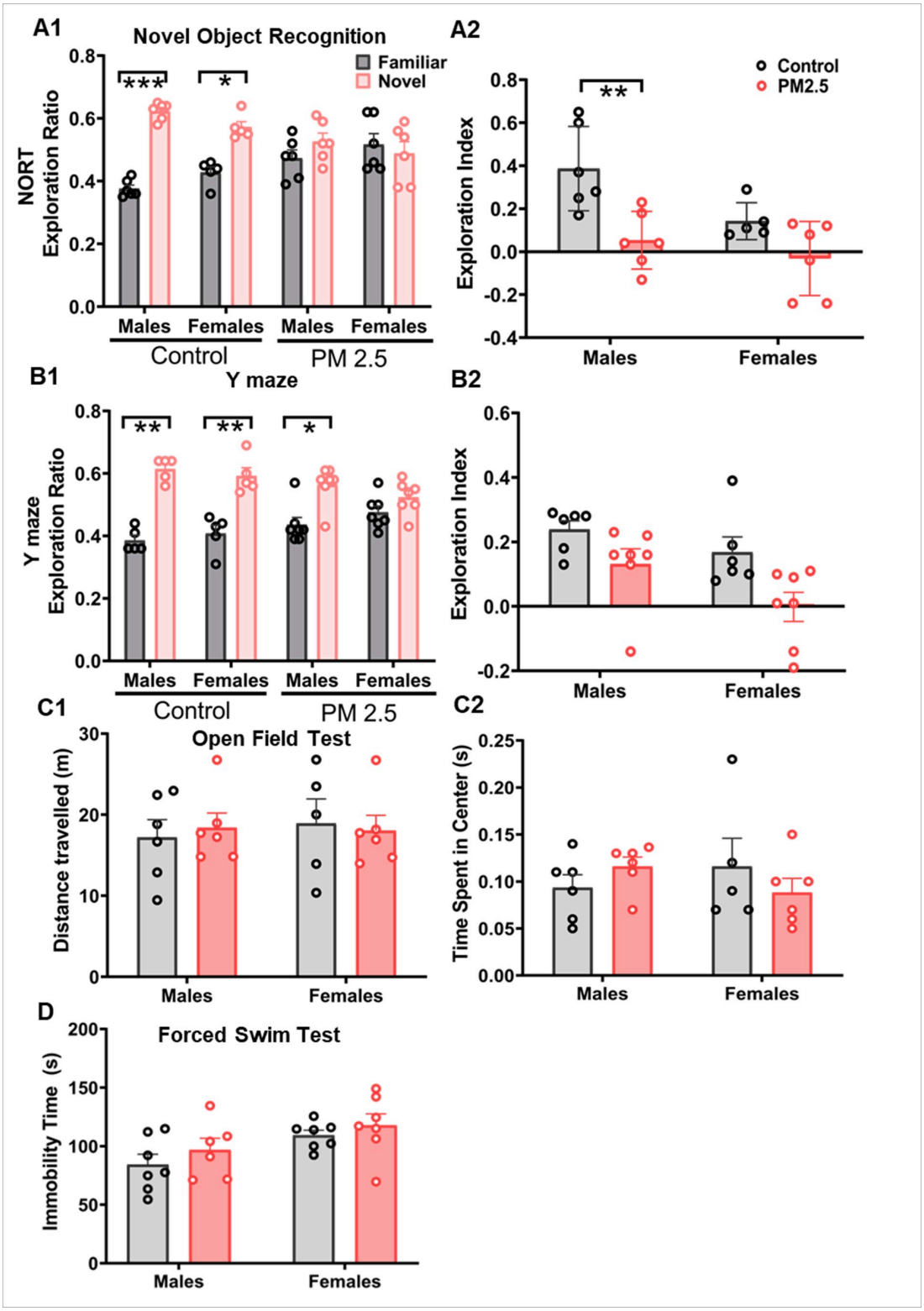


Figure 3

Maternal exposure to $PM_{2.5}$ in impaired working memory in adult male offspring.(A) Working memory was assessed with the novel object recognition (NOR) task (A1) paired t-test: *P < 0.05; **P < 0.01 vs familiar object) , and (B) spatial memory performance was evaluated using the Y-maze task, (B1) exploration ratio: paired t-test: *P < 0.05; ***P < 0.001 vs familiar object). (A2 and B2) the exploration index (males: **P < 0.01) identified via a two-way ANOVA with Tukey's post-hoc test for multiple

comparisons. (C1) Anxiety-like behavior and (C2) locomotor activity were measured in the open field test. (D) Depression-like behavior was evaluated using the forced swim test. Statistical comparisons for panels C and D were performed using a two-way ANOVA followed by Tukey's post-hoc test for multiple comparisons. n = 5–7 mice per group.

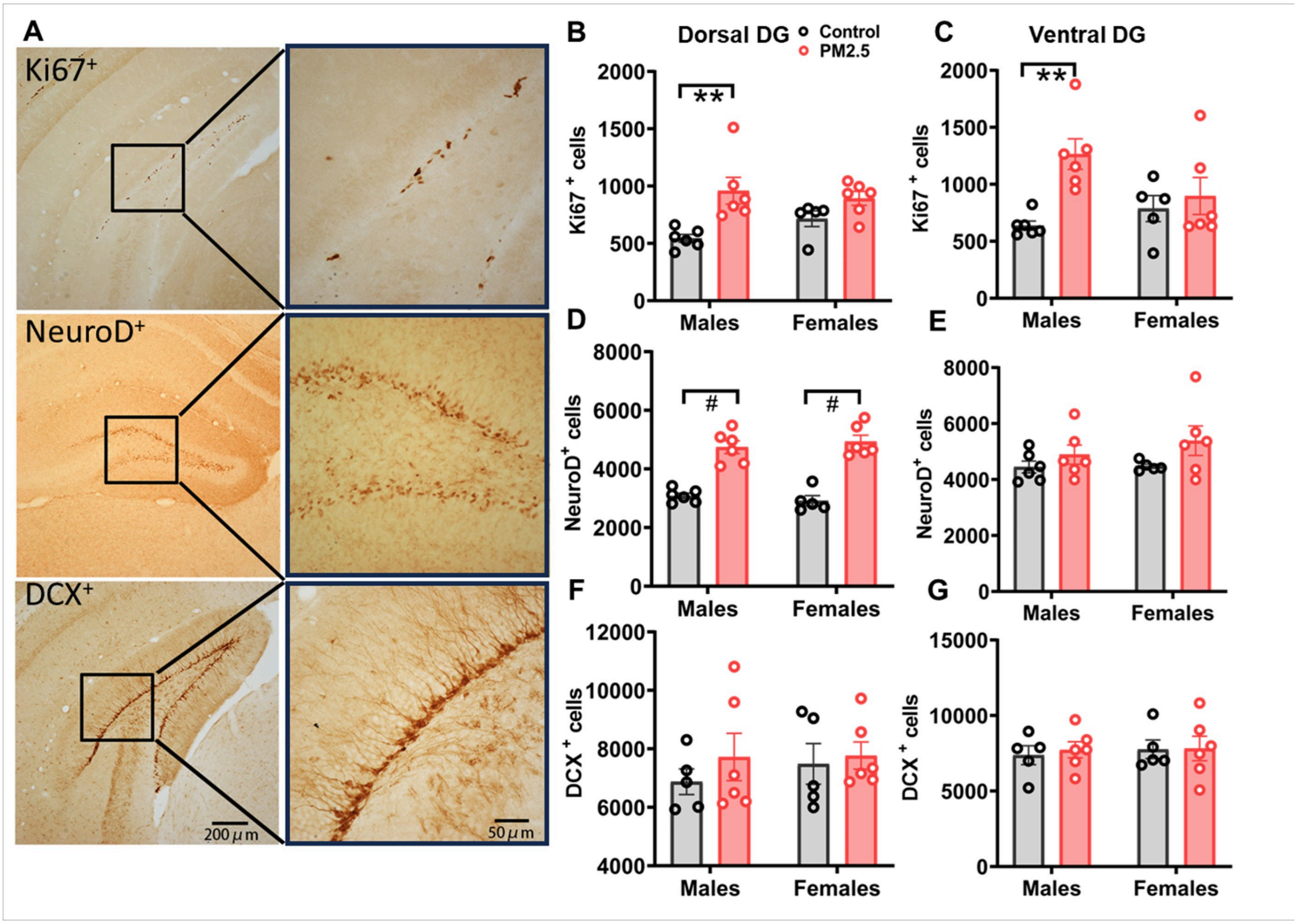


Figure 4

Maternal exposure to $PM_{2.5}$ enhanced hippocampal cell proliferation and neuronal differentiation in male offspring. (A) Representative images of Ki67+, NeuroD+, and DCX+ cells in the hippocampal dentate gyrus at 10 x (scale bar = 200 μm) and 40 x (scale bar = 50 μm) magnification. (B-C) The density of Ki67+ cells in the dorsal and ventral hippocampi. (D-E) The density of NeuroD+ cells in the dorsal and ventral hippocampi. (F-G) The density of DCX+ cells in the dorsal and ventral hippocampus. **P < 0.01 and #P < 0.0001 by two-way ANOVA with Tukey's post-hoc test for multiple comparisons. n = 5–8 mice per group.

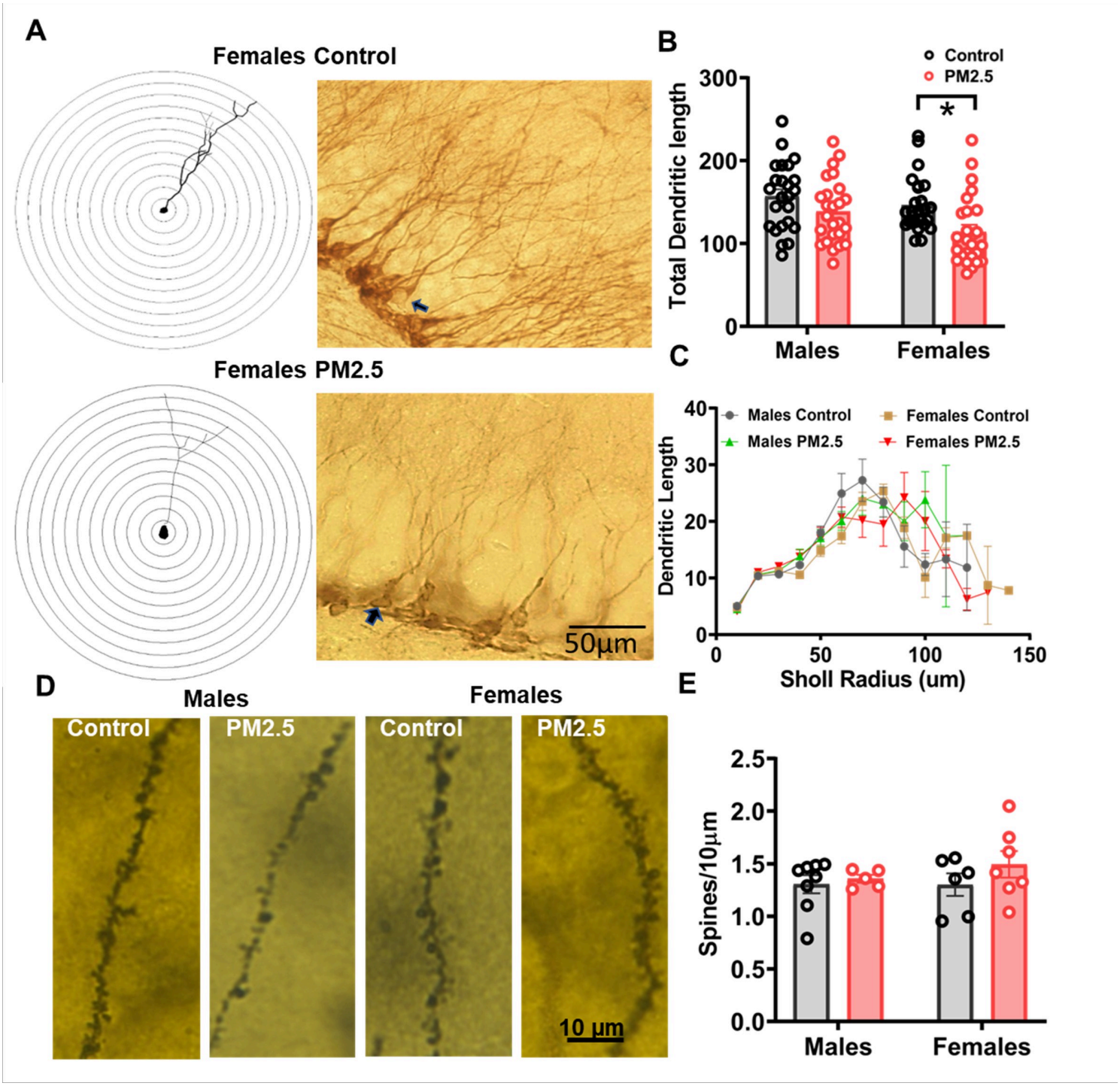


Figure 5

Maternal exposure to $PM_{2.5}$ reduced total dendritic length of immature 1202 adult-born neurons in the hippocampus of female offspring.

(A) Representative images of doublecortin-positive immature neurons in the hippocampus. Scale bar: 50 μm. (B) The total dendritic length of doublecortin-labeled immature neurons. (C) Sholl analysis of dendritic length. (D) Representative images of dendritic spines in the hippocampal dentate gyrus using

Golgi-Cox staining. Scale bar: 10 μm. (E) The density of dendritic spines *P < 0.05 by two-way ANOVA with Tukey's post-hoc test for multiple comparisons. n = 5–8 mice per group.

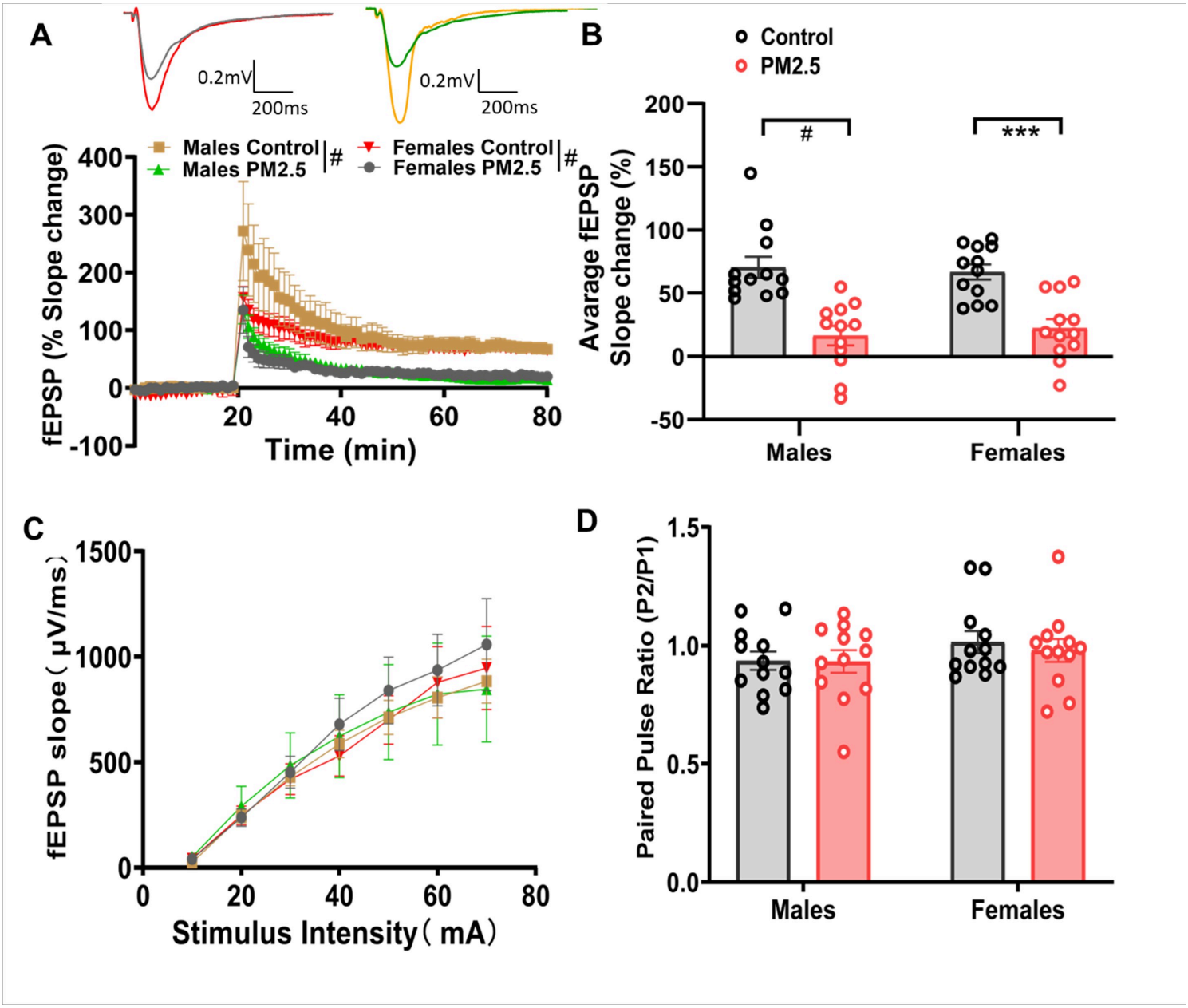


Figure 6

Maternal exposure to $PM_{2.5}$ significantly reduced synaptic plasticity in the 1212 hippocampal dentate gyrus in field electrophysiological recording. (A) Changes in long-term potentiation (LTP) formation. (B) The average slope changes, normalized to baseline, recorded during the last 5 minutes following high-frequency stimulation (HFS; four trains of 0.5 s duration at 100 Hz). (C) The input/output (I/O) curve of the field excitatory postsynaptic potential (fEPSP) slope in response to increasing stimulus intensity. (D) No significant difference in paired-pulse stimulation. Two-way ANOVA with Tukey's post-hoc test for multiple comparisons. ***p < 0.001 and # p < 0.0001. n = 12 slices from 4 mice.

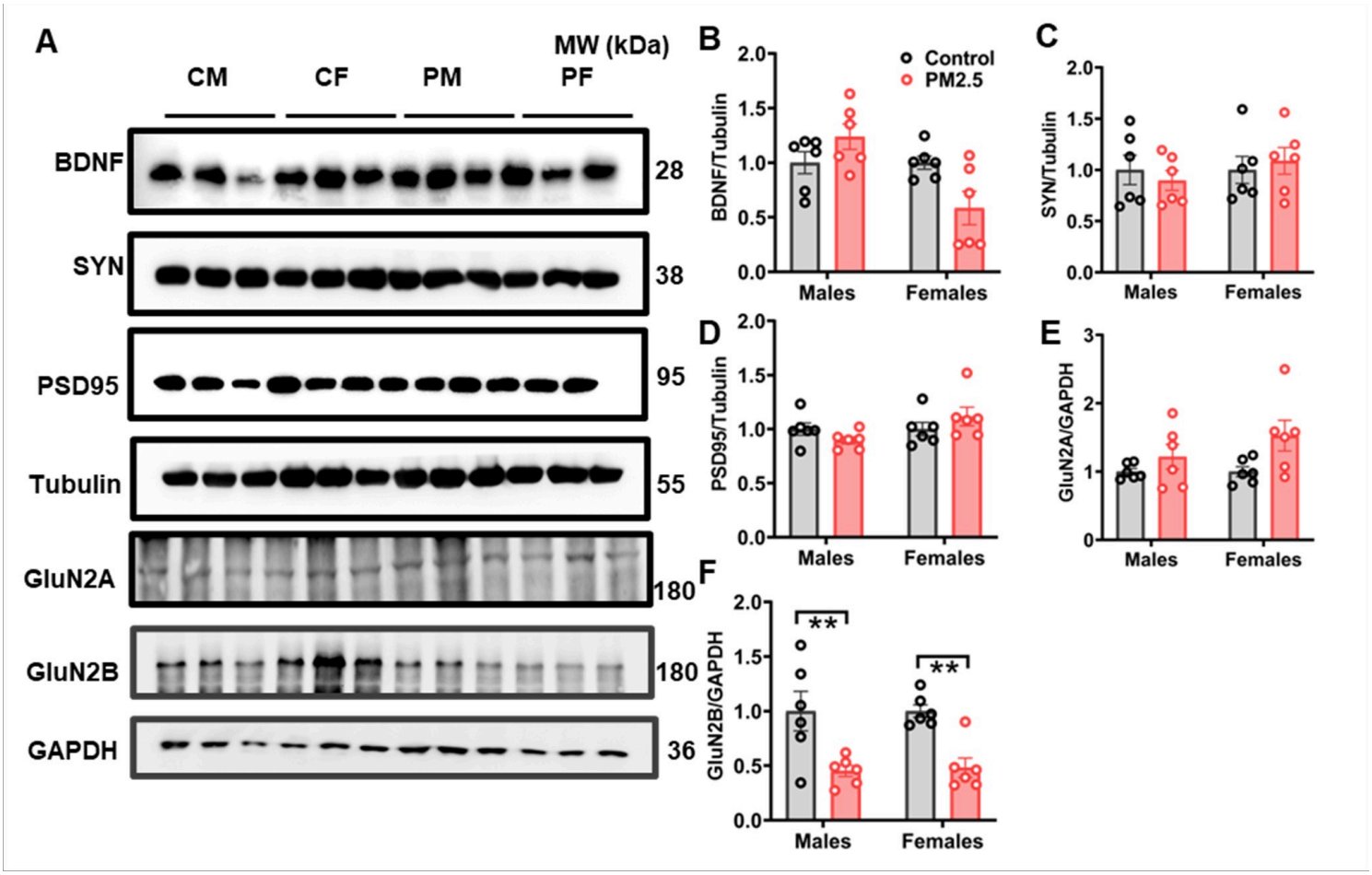


Figure 7

Effects of maternal exposure to $PM_{2.5}$ on hippocampal synaptic protein expression in offspring. (A) Representative images of Western blotting. Quantitative analysis showed no difference in protein expression levels of (B) BDNF, (C) synaptophysin, (D) PSD95, (E) GluN2A, but significant reduction of (F) GluN2B expression levels in hippocampal synaptoneurosome fractions. **p < 0.01, two-way ANOVA with Tukey 1226 post-hoc test for multiple comparisons. n = 6 mice per group.

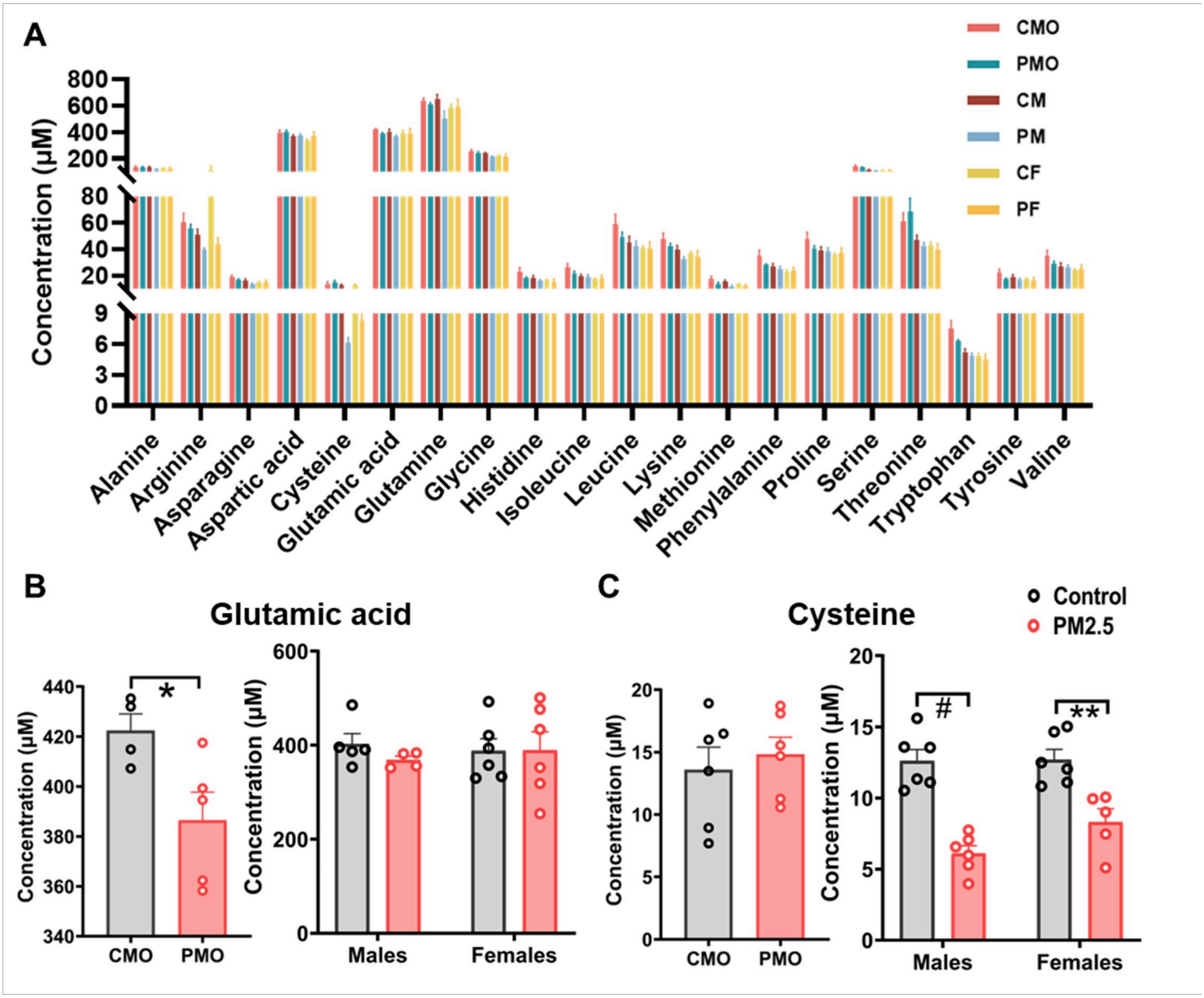


Figure 8

Metabolomic analysis of amino acid levels in the hippocampal tissues of offspring mice. (A) Standard amino acid levels in the hippocampus of maternal and offspring mice. CMO (Control Mother), PMO ($PM_{2.5}$-treated Mother), CM (Male Offspring with Control Mother), PM (Male Offspring with $PM_{2.5}$-treated Mother), CF (Female Offspring with Control Mother), and PF (Female Offspring with $PM_{2.5}$ treated Mother). (B) Glutamic acid concentration in the hippocampi. (C) Cysteine concentration in the hippocampi of offspring mice. Student's T test for two groups and two-way ANOVA with Tukey's post-hoc test for multiple comparisons. n = 4–6 per group. *$p < 0.05$, **$p < 0.01$, and #$p < 0.0001$.

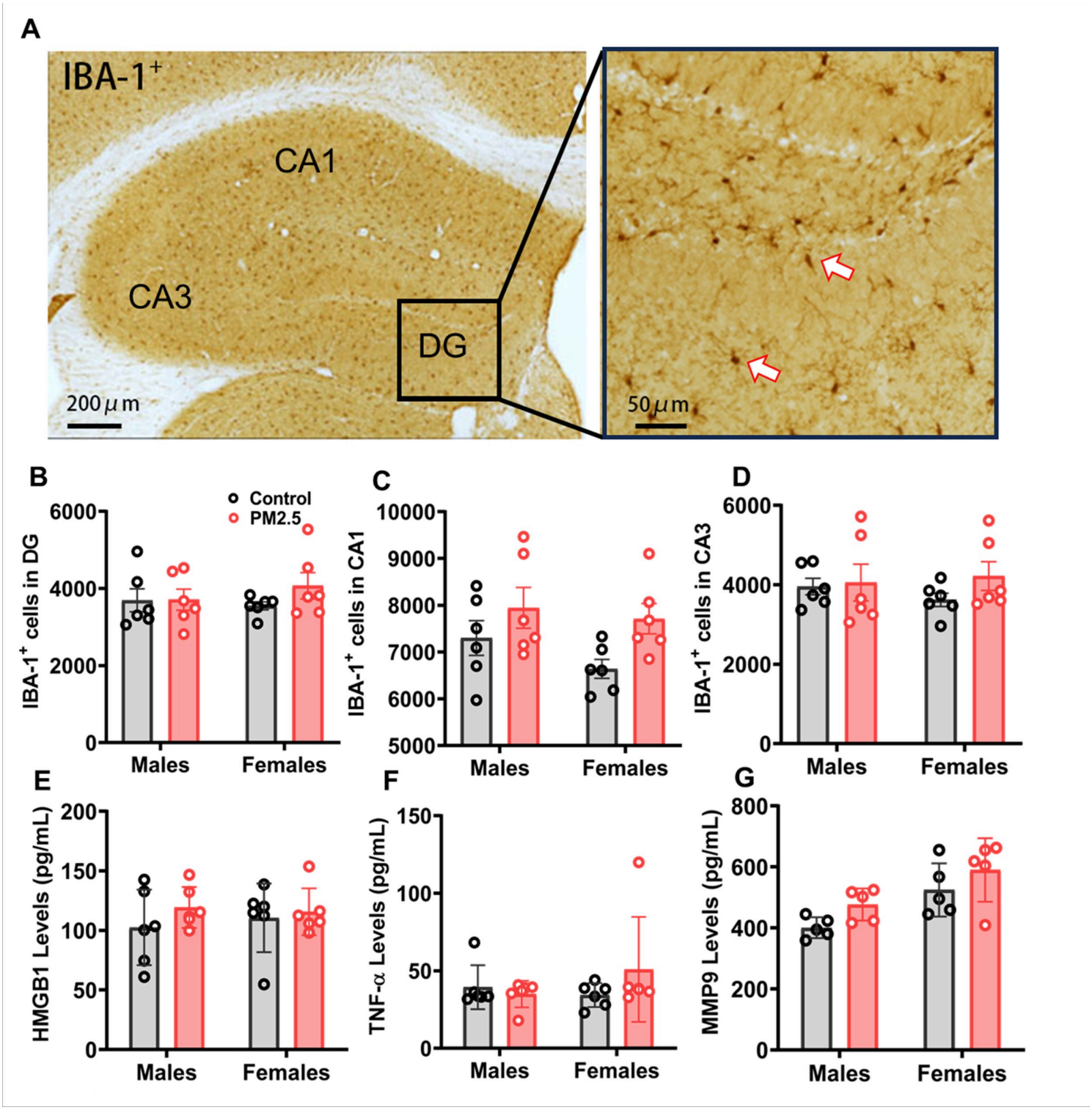


Figure 9

Maternal exposure to $PM_{2.5}$ did not induce neuroinflammation in the hippocampal of offspring. (A) Representative images of Iba-1 positive cells in the hippocampal dentate gyrus. (B-D) Quantification of Iba-1 positive microglial cells in the (B) dentate gyrus (DG), (C) cornu ammonis 1 (CA1), and (D) CA3 regions. (E-G) Levels of inflammatory cytokines in the hippocampi of offspring, including (E) High Mobility Group Box 1 protein (HMGB1), (F) tumor necrosis factor-alpha (TNF-α), and (G) Matrix

Metallopeptidase 9 (MMP-9). Two-way ANOVA with Tukey's post-hoc test for multiple comparisons. n = -6 mice per group.

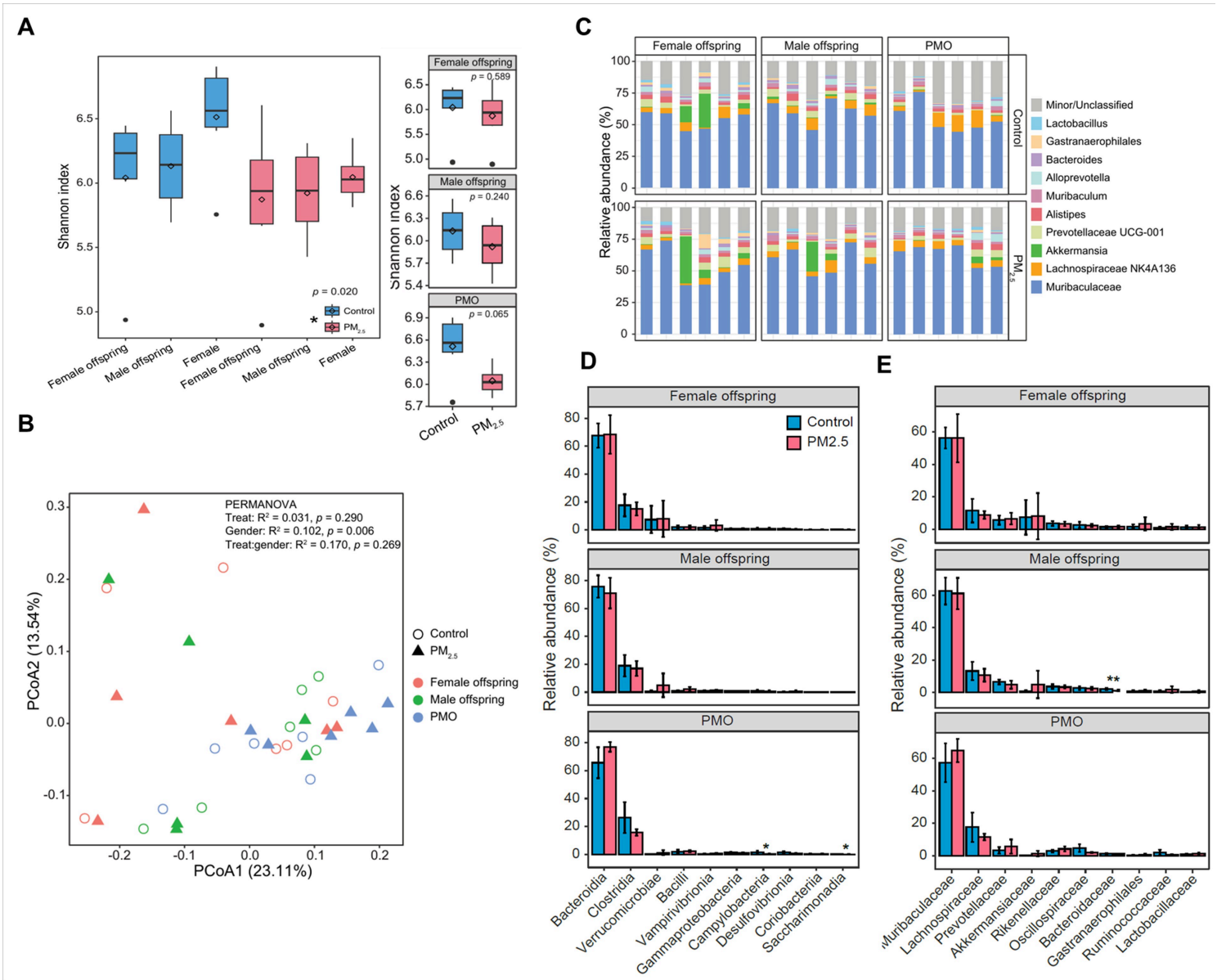


Figure 10

The diversity and composition of fecal microbiota of offspring mice. (A) Alpha-diversity of the fecal microbiota among male offspring, female offspring, and mothers exposed to $PM_{2.5}$(PMO). (B) Principal coordinate analysis (PCoA) of the Bray–Curtis dissimilarity matrix in intestinal microbiota composition. (C) The relative abundance of the top 10 genera in the intestinal microbiota. (D) The relative abundance of the top 10 classes among male offspring, female offspring, and PMO. (E) The relative abundance of the top 10 families among male offspring, female offspring, and PMO. Statistical differences between two groups were determined using the nonparametric Mann-Whitney U test, while differences among more than two groups were assessed using the Kruskal-Wallis test. Both tests were performed in the R package “stats” (v.4.2.2). n = 6 per group. *p < 0.05 and **p < 0.01.